Fermi National Accelerator Laboratory

FERMILAB-Conf-80/79-THY
September 1980

Seven Topics in Perturbative QCD*

ANDRZEJ J. BURAS
Fermi National Accelerator Laboratory
Batavia, Illinois 60510

ABSTRACT

The following topics of perturbative QCD are discussed: 1. Deep inelastic scattering; 2. Higher order corrections to e^+e^- annihilation, to photon structure functions and to quarkonia decays; 3. Higher order corrections to fragmentation functions and to various semi-inclusive processes; 4. Higher twist contributions; 5. Exclusive processes; 6. $p_\perp$ effects; 7. Jet and photon physics.

*Extended version of the invited talk presented at the Symposium on "Topical Questions in QCD", Copenhagen, July, 1980. To be published in Physica Scripta.

Table of Contents

or

ii) we have to show that the following factorization is possible

$$[\text{large distances}] \otimes [\text{short distances}] \qquad (1.1)$$

(examples are the deep-inelastic structure functions, semi- inclusive cross-sections, hadronic formfactors, etc.).

In the first case the relevant quantities can be calculated in perturbation theory in $\alpha(Q^2)$, the effective coupling constant:

i)

$$[\alpha(Q^2)]^N[r_0 + r_1\alpha(Q^2) + r_2\alpha^2(Q^2) + \ldots] + O(\frac{1}{Q^2}) \qquad (1.2)$$

with r_0, r_1, r_2 being calculable in QCD, N being an integer, and Q^2 denoting a large variable. We have for instance (PQ = paraquarkonium)

$$N = \begin{cases} 0 & \text{for } R = \sigma(e^+e^-\to\text{hadrons})/\sigma(e^+e^-\to\mu^+\mu^-) \\ 2 & \text{for } \Gamma(PQ\to\text{hadrons})/\Gamma(PQ\to\gamma\gamma) \\ -1 & \text{for photon structure functions.} \end{cases} \qquad (1.3)$$

In the second case one obtains

ii)

$$\sum_i f_i(x,Q^2) \otimes \sigma_i(x,\alpha(Q^2)) \tag{1.4}$$

where x stands for a fixed ratio of two large invariants, Q^2 is a large variable, and the summation is over quarks, antiquarks and gluons. The "cross-sections" σ_i (short distance functions, coefficient functions) are calculable in perturbative QCD and have expansion in $\alpha(Q^2)$ of the form of Eq. (1.2). On the other hand only the Q^2 evolution of the functions f_i can be calculated by perturbative methods. For instance f_i stand for Q^2 dependent parton distributions or fragmentation functions, and σ_i stand for elementary parton cross-sections to be discussed below.

There is then a hope that at high energies measurable quantities are functions of a few effective <u>universal (process independent)</u> functions:

- effective coupling constant $\alpha(Q^2)$,
- effective parton distributions $q_i(x,Q^2)$, $\bar{q}_i(x,Q^2)$, $G(x,Q^2)$, and fragmentation functions $D_i(z,Q^2)$ in connection with inclusive and semi-inclusive processes,

and

- effective "parton distribution amplitudes" $\phi(x_i,Q^2)$ in the case of exclusive processes.

Now since the coefficients r_i,σ_i of these effective functions are calculable in perturbation theory and are process dependent there is a chance that a finite number of experiments could determine these effective functions, for which only the Q^2 dependence is known. Consequently predictions for other experiments could be made.

This is the program of perturbative QCD. In order to make it meaningful one has to check whether

i) perturbative expansions at present (finite) energies are well behaved, and

whether

ii) $1/Q^2$ effects in (1.2) and (1.4) (so called higher twist effects)

and

iii) non-perturbative (e.g., instanton) effects are small.

In this review we shall discuss in detail point i), summarize the present status of ii), and only say a few words about the non-perturbative effects.

In Section 2, after the recollection of most relevant formulae, we shall list the properties of both the formal and the intuitive approach to deep-inelastic scattering with particular emphasis put on higher order corrections. We shall discuss definition dependence of the effective functions $\alpha(Q^2)$ and $f_i(x,Q^2)$ in some detail. A brief account of the phenomenological applications will also be given in

this section. The material of this section represents our first topic.

In Sections 3 and 4, which take care of the topics 2 and 3, we give an almost complete review of all higher order QCD calculations done so far. Section 3 deals with the quantities of type (1.2), whereas Section 4 discusses the quantities of type (1.4). Regularities in higher order corrections will be emphasized and the methods of dealing with large higher order correction will be briefly reviewed.

In Section 5 we shall summarize our present theoretical and phenomenological knowledge of higher twist contributions. This is our fourth topic.

Section 6 deals with Exclusive Processes. Since at this Symposium this (fifth on our list) topic has been already covered in the talks of Stan Brodsky and Tony Duncan, we shall only present here the basic structure of QCD formulae for the processes in question and list the most striking predictions.

In Section 7, which deals with our sixth topic, we turn to the discussion of $p_\perp$ effects. In addition to large $p_\perp$ effects the recent progress in the understanding of intermediate and small $p_\perp$ physics will be reviewed.

For completeness we shall very briefly discuss in Section 8 jet physics and photon physics.

Finally in Section 9 a summary, an outlook and a list of outstanding questions will be given.

Further details on the topics discussed here can be found in various reviews which are listed in refs.[2-12].

2. Deep-Inelastic Scattering

2.1. Basic Formulae

In QCD and in the leading twist approximation the moments of the deep-inelastic structure functions are given as follows

$$M_k(n,Q^2) = \int_0^1 dx\, x^{n-2}\, \mathcal{F}_k(x,Q^2) \quad k=2,3 \tag{2.1}$$

$$= \sum_{i=NS,S,G} A_n^i(\mu^2)\, C_{k,n}^i\left(\frac{Q^2}{\mu^2}, g^2\right), \tag{2.2}$$

where the functions $\mathcal{F}_k(x,Q^2)$ are related to the standard deep-inelastic structure functions $F_k(x,Q^2)$ by $\mathcal{F}_2=F_2$ and $\mathcal{F}_3=x\,F_3$. In Eq. (2.2) $A_n^i(\mu^2)$ stand for the hadronic matrix elements of non-singlet (NS), singlet (S) and gluon (G) operators and C_n^i are the corresponding coefficient functions in the Wilson operator product expansion. Furthermore g is the renormalized quark-gluon coupling constant and μ^2 is the subtraction scale at which the theory is renormalized. The important property of Eq. (2.2) is the factorization of <u>non-perturbative</u> pieces $A_n^i(\mu^2)$ from <u>perturbatively</u> calculable coefficient functions $C_{k,n}^i(Q^2/\mu^2,g^2)$.

Since A_n^i's are incalculable by present methods, they must be found from the data at some arbitrary (but sufficiently large) value of $Q^2=\mu^2=Q_0^2$.

Specializing Eq. (2.2) to non-singlet structure functions, and using renormalization group equations [2,3] for $C^{NS}_{k,n}\ (Q^2/\mu^2, g^2)$ one obtains

$$M^{NS}_k(n,Q^2) = A^{NS}_n(\mu^2)\exp\left[-\int_{\bar{g}(\mu^2)}^{\bar{g}(Q^2)} dg' \frac{\gamma^{NS}_n(g')}{\beta(g')}\right] * C^{NS}_{k,n}\ (1, g^{-2}(Q^2)) \tag{2.3}$$

$$= A^{NS}_n(\mu^2)\left[\frac{\bar{g}^2(Q^2)}{\bar{g}^2(\mu^2)}\right]^{d^{NS}_n}\left[1 + \frac{\bar{g}^2(Q^2)-\bar{g}^2(\mu^2)}{16\pi^2}\ Z^{NS}_n\right] *$$

$$\left[1 + \frac{\bar{g}^2(Q^2)}{16\pi^2}\ B^{NS}_{k,n}\right] \tag{2.4}$$

where terms of order $\bar{g}^4$ have been neglected.

Furthermore

$$d^{NS}_n = \frac{\gamma^{0,n}_{NS}}{2\beta_0}\ ,\quad Z^{NS}_n = \frac{\gamma^{(1),n}_{NS}}{2\beta_0} - \frac{\gamma^{(0),n}_{NS}}{2\beta_0^2}\ \beta_1\ , \tag{2.5}$$

and $\bar{g}^2$ is the effective coupling constant. In obtaining Eqs. (2.4) and (2.5) the following expansions for the anomalous dimensions (γ^{NS}_n), β function and the coefficient function $C^{NS}_{k,n}(1,\bar{g}^2)$ have been used

$$C^{NS}_{k,n}(1,\bar{g}^2) = \delta^{(k)}_{NS}\left(1 + \frac{\bar{g}^2}{16\pi^2}\ B^{NS}_{k,n} + \ldots\right)\ , \tag{2.6}$$

$$\gamma^n_{NS}(g) = \gamma^{(0),n}_{NS}\ \frac{g^2}{16\pi^2} + \gamma^{(1),n}_{NS}\ \frac{g^4}{(16\pi^2)^2} + \ldots \tag{2.7}$$

$$\beta(g) = -\beta_0 \frac{g^3}{16\pi^2} - \beta_1 \frac{g^5}{(16\pi^2)^2} + \ldots \qquad (2.8)$$

In what follows we shall drop the weak or electromagnetic charge factors $\delta_{NS}^{(k)}$.

Finally the Q^2 evolution of $\bar{g}^2(Q^2)$, corresponding to the β function of Eq. (2.8), is given as follows

$$\frac{\bar{g}^2(Q^2)}{16\pi^2} \equiv \frac{\alpha(Q^2)}{4\pi} = \frac{1-(\beta_1/\beta_0^2)\ln\ln(Q^2/\Lambda^2)/\ln(Q^2/\Lambda^2)}{\beta_0 \ln(Q^2/\Lambda^2)} \,, \qquad (2.9)$$

with Λ being the famous QCD scale parameter. As shown in Table I each of the parameters $\gamma_{NS}^{(o),n}$, $\gamma_{NS}^{(1),n}$, β_0, β_1 and $B_{k,n}^{NS}$ has been calculated [13-22] by at least two groups. Their numerical values and the corresponding analytic expressions are collected in the same notations in refs. [3] and [23].

To proceed further one can use either <u>formal</u> approach or <u>intuitive</u> approach. We begin with the formal approach which we discuss in Section 2.2-2.4. Subsequently we shall deal with the intuitive approach, (Section 2.5).

2.2. <u>Formal Approach</u>

Since the left-hand side of Eq. (2.4) does not depend on μ^2 the r.h.s. of this equation can be put in the following form

$$M_k^{NS}(n,Q^2) = \tilde{A}_n^{NS}\left[\alpha(Q^2)\right]^{d_n^{NS}}\left[1 + \frac{\alpha(Q^2)}{4\pi} R_{k,n}^{NS}\right] \quad , \qquad (2.10)$$

with

$$R_{k,n}^{NS} = Z_n^{NS} + B_{k,n}^{NS} \quad , \qquad (2.11)$$

and $\tilde{A}_n^{NS}$ being independent of μ^2.

Let us list the most important properties of Eqs. (2.10) and (2.11)

a) $\gamma_{NS}^{(1),n}$ and $B_{k,n}^{NS}$ depend on the renormalization scheme [17] used to calculate these quantities. This renormaliation prescription dependence of $\gamma_{NS}^{(1),n}$ and $B_{k,n}^{NS}$ cancel in Eq. (2.11) if these quantities are calculated in the same scheme; i.e. the combination

$$\frac{\gamma_{NS}^{(1),n}}{2\beta_0} + B_{k,n}^{NS} \quad , \qquad (2.12)$$

is renormalization prescription independent. This renormalization prescription dependence of $B_{k,n}^{NS}$ and of $\gamma_{NS}^{(1),n}$ is easy to understand. In order to find $B_{k,n}^{NS}$ one has to calculate [22] both the $\bar{g}^2$ corrections to the virtual Compton amplitude (photon-quark scattering), and the $\bar{g}^2$ corrections to the martix elements of non-singlet operators sandwiched between quark states as illustrated in Fig. 1. Whereas the virtual Compton amplitude is finite and henceforth independent of any renormalization scheme the matrix elements

in question are divergent and have to be renormalized. Different renormalization schemes lead then to different estimates of these matrix elements and consequently to different values for $B^{NS}_{k,n}$. Since the final result for $M^{NS}_k(n,Q^2)$ cannot depend on renormalization scheme, the only way that the renormalization prescription dependence can be cancelled is by that of $\gamma^{(1),n}_{NS}$. This is indeed the case as shown in ref. [17].

b) The coefficients $R^{NS}_{k,n}$ depend on the definition of α[22,24]. If $\alpha(Q^2)$ is redefined to $\alpha'(Q^2)$ with

$$\alpha(Q^2) = \alpha'(Q^2) + r[\alpha'(Q^2)]^2 + 0(\alpha'^3) \ , \qquad (2.13)$$

and r being constant, then the coefficients $R^{NS}_{k,n}$ in Eq. (2.10) are changed to

$$[R^{NS}_{k,n}]' = R^{NS}_{k,n} + 4\pi r \, d^{NS}_n \ . \qquad (2.14)$$

It follows from Eq. (2.14) that the coefficients $R^{NS}_{k,n}$ in Eq. (2.10) have generally two components,

$$R^{NS}_{k,n} = \begin{bmatrix} \text{non-trivial} \\ \text{n dependence} \end{bmatrix} + \begin{bmatrix} \text{trivial n} \\ \text{dependence } \sim d^{NS}_n \end{bmatrix} . \qquad (2.15)$$

Here by "non-trivial" we mean an n dependence different from

d_n^{NS}. The "trivial" component can always be modified by redefining α, whereas the non-trivial part is <u>independent</u> of the definition of α. We shall later discuss efficient methods for comparing the non-trivial n dependence of $R_{k,n}^{NS}$ with the data.

Of course the final answer for $M_k^{NS}(n,Q^2)$ is independent of the definition of $\alpha(Q^2)$ since each change of the coefficients $R_{k,n}^{NS}$ is compensated by the corresponding change of the values of $\alpha(Q^2)$ or equivalently values of Λ extracted from experiment. This is illustrated by the following example.

c) For the $\overline{MS}$ [22] and Momentum Subtraction (MOM) [25,26] schemes, which have been discussed widely in the literature, Eqs. (2.13) and (2.14) read as follows

$$\alpha_{MOM}(Q^2) = \alpha_{\overline{MS}}(Q^2)\left[1 + 1.55\ \beta_0\ \frac{\alpha_{\overline{MS}}(Q^2)}{4\pi}\right], \qquad (2.13')$$

and

$$[R_{k,n}^{NS}]_{\overline{MS}} = [R_{k,n}^{NS}]_{MOM} + \beta_0\ [1.55]\ d_n^{NS}\ . \qquad (2.14')$$

Eq. (2.13') corresponds to the following relation between the scale parameters $\Lambda_{\overline{MS}}$ and Λ_{MOM}:

$$\Lambda_{MOM} = 2.16\ \Lambda_{\overline{MS}}\ . \qquad (2.16)$$

The parameters $R^{NS}_{2,n}$ are plotted as functions of n for the two schemes in question in Fig. 2.

We observe that the coefficients $R^{NS}_{2,n}$ in MOM scheme are smaller than the corresponding parameters in $\overline{MS}$ scheme. However for large n(n>10) both $[R^{NS}_{2,n}]_{\overline{MS}}$ and $[R^{NS}_{2,n}]_{MOM}$ are large and increase as $(\ln n)^2$. In Section 4 we shall discuss methods for dealing with these large corrections.

Having the parameters $R^{NS}_{k,n}$ at hand we could now use Eq. (2.10) to extract $\alpha_{MOM}(Q^2)$ and $\alpha_{\overline{MS}}(Q^2)$ from the data. For pedagogical reasons however we shall proceed differently. As our <u>standard</u> values for Λ_{MOM} and $\Lambda_{\overline{MS}}$ we shall choose the following values

$$\Lambda_{\overline{MS}} = 0.30 \text{ GeV and } \Lambda_{MOM} = 0.55 \text{ GeV} . \qquad (2.17)$$

As shown in Fig. 3 these two values for Λ lead for $Q^2 \geq 10$ GeV^2 to essentially indistinguishable results for $M^{NS}_2(n,Q^2)$ if the corresponding parameters $R^{NS}_{2,n}$ of Fig. 2 are used in Eq. (2.10). We remark that the leading order (L.O.) expression (Eq. 2.10 with β_1 and $R^{NS}_{k,n}$ equal zero) would give a curve similar to the curves in Fig. 3 if the corresponding scale parameter Λ_{LO} was chosen to be $\Lambda_{LO} \approx 0.45$ GeV. This value is consistent with the experimental data.

Furthermore the parameters in Eq. (2.17) are larger only by a factor 2-3 than the corresponding $\Lambda_{\overline{MS}}$ and Λ_{MOM} extracted from the lattice calculations [27]. Inclusion of fermions in the latter calculations would make this difference even

smaller.

Our standard values for $\Lambda_{\overline{MS}}$ and Λ_{MOM} lead through Eq. (2.9) to $\alpha_{\overline{MS}}(Q^2)$ and $\alpha_{MOM}(Q^2)$ which are shown in Fig. 4. For comparison also $\alpha_{LO}(Q^2)$ with Λ_{LO} = 0.40 GeV and Λ_{LO}=0.50 GeV are plotted there. As expected (see (2.13')) $\alpha_{\overline{MS}}(Q^2)<\alpha_{MOM}(Q^2)$. However it is interesting to notice that both $\alpha_{\overline{MS}}$ and α_{MOM} are smaller than the corresponding values of α_{LO} [28]. This is mainly due to the second term in Eq. (2.9). Consequences of this fact will be discussed later on.

An observant reader has noticed that our standard values of Eq. (2.17) do not satisfy Eq. (2.16). This is due to the fact that when we inserted Eq. (2.13') into (2.10) and expanded in powers of $\alpha_{\overline{MS}}$ we consistently neglected terms of $0(\alpha^2_{\overline{MS}})$. Figure 5 shows how the relation (2.16) would be violated if different values for $\Lambda_{\overline{MS}}$ have been used and if the expansion in powers of $1/\ln Q^2/\Lambda^2$ (see (2.19)) instead of the expansion in powers of $\alpha(Q^2)$ has been made in Eq. (2.10). We observe that whereas for $\Lambda_{\overline{MS}}\leq 0.3$ the relation (2.16) is quite well satisfied there are considerable deviations for $\Lambda_{\overline{MS}} > 0.5$. In what follows we shall throughout this paper use the values of Eq. (2.17).

d) It is instructive to calculate the term

$$1 + \frac{\alpha_i(Q^2)}{4\pi}\,[R^{NS}_{2,n}]_i \qquad i = \overline{MS}, MOM\ , \tag{2.18}$$

in Eq. (2.10) which is equal unity in the leading order.

Using our standard values of $\alpha_i(Q^2)$ (Fig. 4) we obtain the curves shown in Fig. 6. We conclude that in the expansion in $\alpha(Q^2)$ the next-to-leading order corrections to $M_2^{NS}(n,Q^2)$ calculated in the MOM scheme of refs. [25,26] are smaller than those in the $\overline{MS}$ scheme. An opposite conclusion is reached in the case of the expansion in the inverse powers of logarithms. This expansion can be obtained from Eqs. (2.10) and (2.9) with the result

$$M_k^{NS}(n,Q^2) = \tilde{A}_n^{NS}\left[\frac{4\pi}{\beta_0 \ln(Q^2/\Lambda_i^2)}\right]^{d_n^{NS}}\left[1 + \frac{R_{k,n}^{NS}(Q^2)}{\beta_0 \ln(Q^2/\Lambda_i^2)}\right], \tag{2.19}$$

where

$$R_{k,n}^{NS}(Q^2) = R_{k,n}^{NS} - \frac{\beta_0}{\beta_0} d_n^{NS} \ln\ln\frac{Q^2}{\Lambda_i^2}. \tag{2.20}$$

The quantity in the last bracket in Eq. (2.19) is plotted in Fig. 7.

e) One may think for a while that there is no point in doing next to leading and higher order calculations since at the end one can anyhow change the size of various terms in the expansion by redefining α. The point is however that by doing consistent higher-order calculations in various processes such as deep-inelastic scattering, $e^+e^-\to$hadrons, photon-photon scattering etc. one can meaningfully compare QCD effects in these processes using one universal effective coupling constant $\alpha(Q^2)$ extracted e.g. from deep-inelastic

scattering data.

By studying higher order corrections to various processes one can hopefully find a universal definition of α for which QCD perturbative expansions are behaving well. Such studies can be found in refs. [29,30]. In this review we shall first present in Sections III and IV all next to leading order corrections in the $\overline{MS}$ and MOM schemes with our standard values of Λ_i of Eq. (2.17). This will allow us to see whether $\alpha_{\overline{MS}}$ and α_{MOM} are good candidates for such a universal definition of the effective coupling constant.

f) We have stated under point b) that $M_k^{NS}(n,Q^2)$ being physical quantities do not depend on the definition of α. On the other hand it should be remembered that different definitions for α lead to different estimates of higher order correction, $0(\alpha^2)$, not included in the analysis. The definition should be preferred for which the convergence of the perturbative expansion is fastest. Since at present no such higher order calculations are known (see point g), various authors have argued in favor of one definition for α or another. For instance Celmaster and Sivers [30] give arguments in favor of the MOM scheme. On the other hand Stevenson [31] suggests a method for finding the optimal scheme for QCD calculations. Here we shall take a different approach (see Section 3) which is as follows.

We have seen that MOM and $\overline{MS}$ schemes with Λ_i of Eq. (2.17) lead to the same prediction for deep-inelastic scattering. The important question is then whether these two

schemes, again with Λ_i of Eq. (2.17), lead also to the same predictions for other processes calculated to the same order in α as deep-inelastic scattering. Possible differences in the predictions would indicate the importance of still higher order corrections and the reliability of our calculations based on truncated perturbative expansion.

g) It should be remarked that attempts have been made [32,33] to estimate α^2 corrections to Eq. (2.10) i.e. coefficients $P^{NS}_{k,n}$ defined by

$$M^{NS}_k(n,Q^2) = \tilde{A}^{NS}_n[\alpha(Q^2)]^{d^{NS}_n}\left[1 + \frac{\alpha(Q^2)}{4\pi} R^{NS}_{k,n} + \frac{\alpha^2(Q^2)}{(4\pi)^2} P^{NS}_{k,n}\right]. \tag{2.21}$$

$P^{NS}_{k,n}$ are given as follows [32]

$$P^{NS}_{k,n} = B^{NS}_{k,n} \cdot Z^{NS}_n + \frac{1}{2}(Z^{NS}_n)^2 - \frac{\beta_1}{2\beta_0} Z^{NS}_n + L^{NS}_{k,n}, \tag{2.22}$$

where

$$L^{NS}_{k,n} = D^{NS}_{k,n} + \frac{\gamma^{(2),n}_{NS}}{4\beta_0} - \frac{\beta_2\gamma^{(0),n}_{NS}}{4\beta_0^2} \quad . \tag{2.23}$$

Here $D^{NS}_{k,n}$, $\gamma^{(2),n}_{NS}$ and β_2 are the coefficients of $(\alpha/4\pi)^2$, $(\alpha/4\pi)^3$ and $g(\alpha/4\pi)^3$ in the expansions (2.6), (2.7) and (2.8) respectively. These coefficients have not been calculated so far. One notes however that if Z^{NS}_n of Eq. (2.5) is inserted into (2.23), seven out of ten terms contributing

to $P^{NS}_{k,n}$ depend only on the known parameters of Table I. One argues then that there is a 30% uncertainty in the estimate of $P^{NS}_{k,n}$. The problem with this argument is that out of the "known" seven terms only two do not depend on the renormalization scheme used to renormalize the local operators (see point a)). The sum of the remaining five is renormalization scheme dependent, and this dependence has to be cancelled by that of $L^{NS}_{k,n}$. The $L^{NS}_{k,n}$ are however unknown. In summary we think that little is known about the size of the coefficients $P^{NS}_{k,n}$[34], except maybe for large values of n as discussed in Section IV.

h) The novel feature of next to leading order corrections is the following n dependence of $\gamma^{(1),n}_{NS}$ [17,35]

$$\gamma^{(1),n}_{NS} = \gamma^{\alpha}_{n} + (-1)^{n}\,\gamma^{\beta}_{n}\ , \tag{2.24}$$

where γ^{α}_{n} and γ^{β}_{n} may be analytically continued in n. Consequently the even and odd values of $\gamma^{(1),n}_{NS}$ must be (for instance in the process of moment inversion) analtically continued to $\gamma^{\alpha}_{n} + \gamma^{\beta}_{n}$ and $\gamma^{\alpha}_{n} - \gamma^{\beta}_{n}$ respectively. This also implies that

$$R^{NS}_{k,n} = \begin{cases} R^{\alpha}_{n} + R^{\beta}_{n} & n \text{ even} \\ R^{\alpha}_{n} - R^{\beta}_{n} & n \text{ odd} \end{cases} \tag{2.25}$$

where the notation is obvious. The fact that $R^{\beta}_{n} \neq 0$ is related

to the occurance of quark→antiquark transitions [35,18] which take place at the two-loop level (see Fig. 8) in addition to quark→quark transitions. Taking into account the crossing properties of various structure functions (see Eq. (2.124) of ref. [3]) one finds for instance, that due to R_n^β being non-zero the combinations $F_2^{ep} - F_2^{en}$ and $F_2^{\nu p} - F_2^{\bar{\nu} p}$ evolve differently with Q^2. In particular the intergral

$$\int_0^1 \frac{1}{x} \left[F_2^{ep} - F_2^{eN} \right] , \tag{2.26}$$

depends weakly on Q^2, whereas

$$\int_0^1 \frac{1}{x} \left[F_2^{\nu p} - F_2^{\bar{\nu} p} \right] = 2 , \tag{2.27}$$

i.e. Adler sum rule is satisfied. The effect in question is however very small [36] and in most applications can be totally neglected. For instance the integral of Eq. (2.26) changes by 0.5% in the range of Q^2 from 5 GeV^2 to ∞! Even smaller effect is found for $n \geq 2$.

i) Since [22,37]

$$R_{3,n} = R_{2,n}^{NS} - \frac{4}{3} \frac{4n+2}{n(n+1)} , \tag{2.28}$$

the Q^2 evolutions of the structure functions F_2^{NS} and F_3 differ slightly from each other beyond the leading order. We

shall discuss this difference in Section 2.5.

j) Finally Quantum Chromodynamics predicts [22] a weak violations of various parton model sum rules such as Gross-Llewellyn-Smith, Bjorken, and Callan-Gross relations. Explicit formulae can be found in Section 2.3 of ref. [3].

This completes the listing of the main properties of Eq. (2.10). We shall now turn to a brief account of the phenomenological tests of this equation.

2.3 Brief Comparison with Data

Equation (2.10) can be directly compared with the experimental data. It is however often useful to use (2.10) to construct quantities which are insensitive to the definition of α and which exhibit a "non-trivial" n dependence (see Eq. (2.15)) of next to leading order corrections. We shall discuss here two such quantities.

One can use formula (2.10) to construct the following ratio [38]

$$P_n^m \equiv \frac{d[\ln M_k^{NS}(m,Q^2)]}{d[\ln M_k^{NS}(n,Q^2)]} = \frac{d_m^{NS}}{d_n^{NS}}\left[1 + \frac{1}{\beta_0 \ln(Q^2/\Lambda^2)}\left(\frac{R_{k,m}^{NS}}{d_m^{NS}} - \frac{R_{k,n}^{NS}}{d_n^{NS}}\right)\right] \quad (2.29)$$

where "d" on the L.h.s. of this Equation stands for the derivative with respect to $\ln Q^2$. The coefficients of $1/(\beta_0 \ln(Q^2/\Lambda^2))$ obviously (see Eq. (2.14)) do not depend on the definition of α. Equation (2.29) is compared with the data in Table II, where also the leading order prediction,

$P_n^m = d_m^{NS}/d_n^{NS}$, is shown. We observe that the next-to leading order corrections improve the agreement of the theory with data.

One can rewrite Eq. (2.10) as follows [24,22,40]

$$M_k^{NS}(n,Q^2) = \tilde{A}_n^{NS}\left[\frac{4\pi}{\beta_0 \ln(Q^2/\Lambda_n^2)}\right]^{d_n^{NS}}\left[1 - \frac{\beta_1}{\beta_0^2}\frac{\ln\ln(Q^2/\Lambda_n^2)}{\ln(Q^2/\Lambda_n^2)}\right]^{d_n^{NS}}, \quad (2.30)$$

where

$$\Lambda_n^{(k)} = \Lambda \exp\left[\frac{R_{k,n}^{NS}}{2\beta_0 d_n^{NS}}\right]. \quad (2.31)$$

The n dependence of $\Lambda_n^{(k)}$ is independent of the definition of α. $\Lambda_n^{(k)}$ increases roughly by factor 2 and 3 for F_2^{NS} and F_3 structure functions respectively if n is varied from n=2 to n=8. In the leading order Λ is independent of n. As shown in Fig. 9 the n dependence of $\Lambda_n^{(k)}$ as given by Eq. (2.31) is in a very good agreement [39-41] with the experimental data [42-44] indicating the importance of next to leading order corrections. This is seen especially for $\Lambda_n^{(2)}$.

2.4 Singlet Structure Functions Beyond the Leading Order

The study of next to leading order QCD corrections to the singlet structure functions is much more complicated than for the non-singlet structure functions due to the mixing between fermion singlet and gluon operators which enter Eq. (2.2). The derivation of formal expressions analogous to

Eq. (2.10) can be found in ref. [3]. Here we shall only make a few remarks.

i) The analysis of singlet contributions requires the calculation of the two-loop anomalous dimension matrix and of the one loop corrections to the fermion singlet and gluon Wilson coefficient functions $C^S_{k,n}(1,\bar{g}^2)$ and $C^G_{k,n}(1,\bar{g}^2)$. As in the non-singlet case, one has to take care that all these quantities are calculated in the same renormalization scheme. First calculations of these quantities have been done in refs. [20,22]. The calculation of the two-loop anomalous dimension matrix performed in ref. [20] is particularly complicated.

ii) It turns out that the formal expressions for the moments of singlet structure functions are very simple [45] e.g.

$$M_2^S(n,Q^2) = \tilde{A}_n^+ \left[\alpha(Q^2)\right]^{d_n^+} \left[1 + \frac{\alpha(Q^2)}{4\pi} R_{2,n}^+\right] + \tilde{A}_n^- \left[\alpha(Q^2)\right]^{d_n^-} \left[1 + \frac{\alpha(Q^2)}{4\pi} R_{2,n}^-\right] \tag{2.10'}$$

where $d_n^\pm$ and $R_{2,n}^\pm$ are known and $\tilde{A}_n^\pm$ have to be extracted from the data. The next to leading order corrections to the singlet structure functions turn out to be of the same order as in the non-singlet sector although their n dependence in particular at low values of n is different due to the mixing. Numerical estimates of these corrections are given in ref. [45],[46].

2.5 Intuitive Approach

2.5.1 Non-Singlet Sector. So far our discussion of deep-inelastic scattering was very formal. We shall now express Eq. (2.4) in terms of parton distributions and parton cross-sections. Let us first recall that the parametrization of the QCD prediction (2.10) in terms of an effective $\alpha(Q^2)$ and explicit higher order corrections ($R^{NS}_{k,n}$) depends on the definition of $\alpha(Q^2)$. Similarly the parametrization of QCD predictions in terms of "effective" parton distributions and parton cross-sections depends on the definition of parton distributions. We shall discuss here two examples.

i) Definition A [47]

One writes Eq. (2.4) as follows

$$M^{NS}_k(n,Q^2) = \langle q^{NS}(Q^2)\rangle^{(a)}_n \cdot \sigma^{NS}_{k,a}(n,\alpha(Q^2)) \ , \qquad (2.32)$$

where

$$\langle q^{NS}(Q^2)\rangle^{(a)}_n = \int_0^1 dx\ x^{n-1} q^{NS}_a(x,Q^2) = A^{NS}_n(Q^2)$$

$$= \langle q^{NS}(Q_0^2)\rangle^{(a)}_n \left[\frac{\bar{g}^2(Q^2)}{\bar{g}^2(Q_0^2)}\right]^{d^{NS}_n} \left[1 + \frac{\bar{g}^2(Q^2)-\bar{g}^2(Q_0^2)}{16\pi^2} Z^{NS}_n\right] \qquad (2.33)$$

are the moments of an effective Q^2 dependent non-singlet parton distribution $q^{NS}_a(x,Q^2)$, and

$$\sigma^{NS}_{k,a}(n,\alpha(Q^2)) = \int_0^1 dx\ x^{n-2}\ \sigma^{NS}_{k,a}(x,\alpha(Q^2))$$

$$= 1 + \frac{\alpha(Q^2)}{4\pi}\ B^{NS}_{k,n}\ , \qquad (2.34)$$

may be regarded as the moments of the elementary parton cross-section. Equation (2.32) is illustrated schematically in Fig. 10. The index "a" distinguishes the definition of parton distributions in question from the second definition, which is discussed below. Furthermore in order to unify notations we have put $\mu^2=Q_0^2$. Note that in this definition the moments of $q^{NS}(x,Q^2)$ are equal to matrix elements of a non-singlet operator normalized at Q^2. Equation (2.32) can be inverted to give

$$F^{NS}_k(x,Q^2) = \int_x^1 \frac{d\xi}{\xi}\ [\xi q^{NS}_a(\xi,Q^2)]\sigma^{NS}_{k,a}\ (\frac{x}{\xi},\alpha(Q^2))\ . \qquad (2.35)$$

Exact analytic expressions for $\sigma^{NS}_{k,a}(x/\xi,\alpha(Q^2))$ can be found in in refs. [48,49]. Approximate analytic expressions for $\xi\ q^{NS}_a(\xi,Q^2)$ will be discussed below.

ii) Definition B [37]

Here the full next-to leading order correction to F_2^{NS} is absorbed into the definition of parton distributions. Equations (2.32)-(2.34) are replaced by

$$M_k^{NS}(n,Q^2) = \langle q^{NS}(Q^2)\rangle_n^{(b)} \sigma_{k,b}^{NS}(n,\alpha(Q^2)) \qquad (2.32')$$

$$\langle q^{NS}(Q^2)\rangle_n^{(b)} = \langle q^{NS}(Q_0^2)\rangle_n^{(b)} \left[\frac{\bar{g}^2(Q^2)}{\bar{g}^2(Q_0^2)}\right]^{d_n^{NS}} \left[1 + \frac{\bar{g}^2(Q^2)-\bar{g}^2(Q_0^2)}{16\pi^2} R_{2,n}^{NS}\right], \qquad (2.33')$$

and

$$\sigma_{k,b}^{NS}(n,\alpha(Q^2)) = \begin{cases} 1 \quad , \quad k = 2 \\ 1 + \frac{\alpha(Q^2)}{4\pi}(B_{3,n}^{NS} - B_{2,n}^{NS}), \quad k=3 \end{cases} \qquad (2.34')$$

respectively. Again exact analytic expressions for $\sigma_{k,b}^{NS}(x/\xi,\alpha(Q^2))$ can be found in ref. [48,49] and the approximate analytic expressions for $\xi\, q_b^{NS}(\xi,Q^2)$ will be discussed below.

Let us list some of the properties of both definitions of parton distributions.

i) the parton distributions defined by Eq. (2.33') are renormalation prescription independent. On the other hand, since Z_n^{NS} and $B_{k,n}^{NS}$ are separately renormalization prescription dependent so are the parton distributions defined by Eq. (2.33).

ii) the renormalization prescription dependence of parton distributions in the case of definition A can be used to find a renormalization scheme for which the evolution equations (2.33) are particularly simple. This turns out to be $\overline{MS}$ scheme for which the parameters Z_n^{NS} are very small [3,49]

$$z_n^{NS} = 1.5 - 2.5 \quad 2 \leq n \leq 8 \ . \tag{2.36}$$

Thus in the case of $\overline{MS}$ scheme the evolution equations for $q_a^{NS}(x,Q^2)$ are essentially the same as the leading order equations [50] except for the modified evolution of the effective coupling constant (see Eq. 2.9). The evolution equations (2.33') in the case of definition B differ substantially at large n (large x) form the leading order equations due to the large values of $B_{k,n}$ for large n and due to the non-trivial behaviour $B_{k,n} \sim (\ln n)^2$.

ii) Whereas the input parton distributions or input structure functions at some $Q^2=Q_0^2$ in the case of the def. B will be for F_2^{NS} the same as in the leading order (i.e. the data does not change) the input distribution in the def. A will differ considerably at low Q^2 and large x from those used in the leading order phenomenology. The reason is that B_n's differ considerably from 1 for low Q^2 and large n.

Of course the final results for the structure functions should be independent of any particular difinition since the differences in the the parton distributions q_a^{NS} and q_b^{NS} will be compensated by the corresponding differences in the parton cross-section σ_a^{NS} and σ_b^{NS}. A detailed study of the effects discussed here has been done in ref. [49]. It turns out that in the range $5 \leq Q^2 \leq 200$ GeV^2 and $0.02 \leq x \leq 0.8$ one can

find simple parametrizations for both definitions of parton distributions which represent to a high accuracy the Eqs. (2.33) and (2.33').

These parametrizations are of the form of leading order parametrizations of ref. [51] i.e.

$$x\, q^{NS}(x,Q^2) \sim x^{\eta_1(\bar{s})}\,(1-x)^{\eta_2(\bar{s})} \tag{2.37}$$

where

$$\eta_i(\bar{s}) = \eta_i^0 + \eta_i'\,\bar{s}\ , \tag{2.38}$$

and

$$\bar{s} = -\ln\left[\frac{\alpha(Q^2)}{\alpha(Q_0^2)}\right]. \tag{2.39}$$

The parameters η_i^0 are to be found from the data at some $Q^2=Q_0^2$. The "slopes" η_i' are on the other hand predictions of the theory. It should be however remembered that η_i''s depend weakly on η_i^0 and Λ. A detailed procedure for finding η_i''s for given input values η_i^0 and Λ can be found in ref. [49,51]. Finally it should be remarked that the method of ref. [49,51] can be trivially extended to the input distributions at $Q^2\neq Q_0^2$ of the form

$$\sum_i A_i\, x^{B_i}(1-x)^{C_i}\ . \tag{2.40}$$

In accordance with points ii) and iii) one has

$$[\eta_i^0]_{LO} = [\eta_i^0]_b \neq [\eta_i^0]_a \ , \tag{2.41}$$

and

$$[\eta_i']_{LO} \lesssim [\eta_i']_a \neq [\eta_i']_b \ , \tag{2.42}$$

where the indices LO, a and b stand for leading order, the definition A and the definition B respectively. For instance $[\eta_2^0]_b$=2.71 and $[\eta_2^0]_a$=3.40 whereas $[\eta_2']_a$=0.76 and $[\eta_2']_b$=1.5.

On the level of structure functions themselves two main properties of the next to leading order corrections are worth-while mentioning [49].

i) If $\Lambda_{\overline{MS}}$ is chosen so that $\Lambda_{\overline{MS}}=\Lambda_{LO}$, where Λ_{LO} is the scale in the leading order expression ($B_n^{NS}=0$, $z_n^{NS}=0$) then a stronger increase (decrease) of structure functions at small (large) values of x is predicted by next-to leading order corrections relative to L.O. predictions.

If $\Lambda_{\overline{MS}}$ is decreased so that scaling violations for $0.4 \leq x \leq 0.7$ are similar to those predicted by leading order formula still some additional increase due to next-to-leading corrections is seen at small x. This non-trivial x dependence of next to leading order corrections is related to the non-trivial n dependence of Λ_n in (Eq. 2.31).

ii) The increase at small x in question is more pronounced for F_3 than F_2^{NS}.

There is some indication that this additional increase in F_3 at small x has been seen in the data [52]. Detailed comparison should however also include charm production effects [53] in F_3 which are of order $(m_c^2-m_s^2)/Q^2$ with m_c and m_s being charm and strange quark mass respectively.

2.5.2 Singlet Sector. In the case of the singlet structure functions the arbitrariness in the definition of parton distributions is twofold. There are two subprocesses contributing: photon-quark and photon-gluon scattering. Within each subprocess there is the arbitrariness of the type discussed for non-singlet parton distributions. Furthermore due to the mixing between quark and gluon operators the separation of the full deep-inelastic process into quark and gluon subprocesses depends on the definition of parton distributions. For instance the Q^2 evolution of singlet quark distributions depends on the definition of gluon distributions and vice versa.

The analogs of definitions A and B of section 2.5.1 are for the singlet parton distributions as follows

i) Definition A

$$M_2^s(n,Q^2) = A_n^s(Q^2)\cdot C_{2,n}^s(1,\bar{g}^2) + A_n^G(Q^2)\cdot C_{2,n}^G(1,\bar{g}^2)$$

$$\equiv <q^s(Q^2)>_n^{(a)}\cdot\sigma_a^s(n,\alpha(Q^2))+<G(Q^2)>_n^{(a)}\cdot\sigma_a^G(n,\alpha(Q^2)) \ , \qquad (2.43)$$

where

$$\langle q^S(Q^2)\rangle_n^{(a)} \equiv A_n^S(Q^2) \text{ and } \langle G(Q^2)\rangle_n^{(a)} = A_n^G(Q^2) \ , \qquad (2.44)$$

are the moments of the effective, Q^2 dependent, singlet quark and gluon distributions, $q_a^S(x,Q^2)$ and $G_a(x,Q^2)$, respectively.

$$\sigma_a^S(n,\alpha(Q^2)) \equiv C_{2,n}^S(1,\bar{g}^2) \text{ and } \sigma_a^G(n,\alpha(Q^2)) \equiv C_{2,n}^G(1,\bar{g}^2) \qquad (2.45)$$

are the corresponding parton cross-sections. Equation (2.43) can be inverted to give

$$F_2^S(x,Q^2) = \int_x^1 \frac{d\xi}{\xi}\left[\xi\, q_a^S(\xi,Q^2)\sigma_a^S\left(\frac{x}{\xi},\alpha(Q^2)\right) + \xi\, G_a(\xi,Q^2)\sigma_a^G\left(\frac{x}{\xi},\alpha(Q^2)\right)\right] \ . \qquad (2.46)$$

Exact analytic expressions exist for σ_a^S and σ_a^G [48]. The evolution equations for $q_a^S(\xi,Q^2)$ and $G_a(\xi,Q^2)$ can be found in refs. [3,54,55]. They are a straightforward generalization of the familiar leading order equations [50]. Furthermore in the $\overline{MS}$ scheme these equations do not differ substantially from the leading order ones.

ii) Definition B

Here the full next-to leading order corrections to

F_2^S is absorbed into the definition of parton distributions, i.e.

$$M_2^s(n,Q^2) = \langle q^s(Q^2)\rangle_n^{(b)} \cdot 1 \qquad (2.47)$$

As discussed in ref. [20] this equation defines also $\langle G(Q^2)\rangle_n^{(b)}$. The evolution equations for $q_a^s(x,Q^2)$ and $G_b(x,Q^2)$ are rather involved. They can be found in ref. [20].

The important lesson which we draw from this section is that since the separate quark and gluon contributions are definition dependent, both have to be taken consistently into account before a physical answer for F_2^S is obtained.

2.6 Miscellaneous Remarks

i) It should be remarked that in ref. [39,56,57] fits of of structure functions or their moments to the data have been made with the general conclusion that the next to leading order corrections improve the agreement of QCD with the data.

ii) A message to our experimental colleques: in refs. [39],[49],[56], simple inversion methods of moments of structure functions or parton distributions with next to leading order corrections included, have been developed. Therefore the analysis of structure functions beyond the leading order should be now as easy as in the leading order. These methods devide into four

classes. In refs. [39] and [49] various explicit parametrizations of the effective parton distributions have been given. One of these parametrizations has been discussed in Section 2.5. Another method is to write $F(x,Q^2)$ as follows

$$F(x,Q^2) = \int_x^1 dy\ K(x,y,Q^2,Q_0^2)\ F(y,Q_0^2)\ , \qquad (2.48)$$

and find analytic expressions for the kernel $K(x,y,Q^2,Q_0^2)$. This method has a slight advantage over the previous method in that the input distribution can be parametrized at will. For the leading order this method has been discussed in ref. [58] and ref. [59] for the non-singlet and singlet structure functions respectively. Generalization of the kernels K( ) beyond the leading order has been given in ref. [56]. Still other methods are discussed in ref. [60]. Finally the evolution equations for parton distributions can be integrated numerically. All methods lead within a few percent of accuracy to the same results.

iii) It has been suggested in ref. [61] to use the moments

$$B_{M,N}(Q^2) = \frac{(M+N+1)!}{M!N!} \int_0^1 x^N(1-x)^M F(x,Q^2)\ dx\ , \qquad (2.49)$$

rather than the moments of Eq. (2.1), which for N>4 are

mostly sensitive to $x>0.5$. With increasing M the moments of Eq. (2.49) become sensitive to small values of x and are particularly well suited for the study of gluon and sea distributions which are concentrated at small values of x.

iv) The next to leading order QCD corrections to the Q^2 evolution of the polarized deep-inelastic structure functions have been calculated in ref. [62]. This generalizes previous leading order studies of Ahmed and Ross [63] and of Altarelli and Parisi [50]. It would be interesting to make one day a phenomenological study of these corrections.

v) There is the outstanding question of calculating the x dependence of structure functions at fixed value of Q^2. This has been addressed in the context of specific models in refs. [64] and [65].

vi) In this review we shall not discuss neither target mass effects nor heavy quark effects. Recent discussions of these topics can be found in refs. [53],[66],and [67], where references to older papers can be found.

vii) Recent discussions of longitudinal structure functions can be found in refs. [68]-[71].

2.7 Summary

A lot has been learned in the last few years about higher order QCD corrections to deep-inelastic scattering. These corrections turn out to improve the argreement of the theory with data. There are however still many problems to be solved on both experimental and theoretical level. First there is the question of the importance of higher twist contributions which we have not discussed so far. We shall return to this question in Section V. Secondly the high Q^2 experiments do not completely agree on the size of scaling violations. In particular the CDHS and BEBC groups (ν experiments) find the parameter $\Lambda_{LO} \lesssim 0.3\text{-}0.5$ GeV, whereas the recent μ-experiments [72] prefer $\Lambda_{LO} < 0.2$ GeV. Are these differences related to experimental problems or maybe to different physics in ν and μ initiated processes [73], explanation of which lies outside the QCD framework? Answer to this question would surely improve our understanding of scaling violations.

For the time being we shall continue our review by turning to other processes, while keeping in mind the lessons of this section.

3. Review of Higher Order Corrections I

In this section we shall discuss the next to leading order correction to three quantities for which at high energies the expansion (1.2) is valid. These are

i) The ratio

$$R^{e^+e^-} = \frac{\sigma(e^+e^- \to \text{hadrons})}{\sigma(e^+e^- \to \mu^+\mu^-)} \quad , \tag{3.1}$$

ii) Photon structure functions,

and

iii) Various ratios in quarkonium decays of which

$$P = \frac{\Gamma(PQ \to \text{hadrons})}{\Gamma(PQ \to \gamma\gamma)} \quad , \tag{3.2}$$

with PQ standing for paraquarkonium, is a well known example.

The parameters r_i of Eq. (1.2) are calculable in QCD. Therefore since we have already "extracted" the values of $\alpha_{\overline{MS}}$ and α_{MOM} or equivalently $\Lambda_{\overline{MS}}$ and Λ_{MOM} (see Eq. 2.17) from deep-inelastic data we can immediately make QCD predictions for the quantities above. In what follows we shall ask two questions:

a) How large are the next to leading order QCD corrections to i)-iii) in $\overline{MS}$ and MOM schemes of Section 2, and

b) Do both schemes (with Λ_i of Eq. 2.17) lead to the same final answers for the quantities above?

3.1 $e^+e^-\rightarrow$hadrons

In the simple parton model and in QCD one obtains for $Q^2 \equiv E^2_{c.m.} \rightarrow \infty$

$$R_\infty^{e^+e^-} = 3 \sum_i e_i^2 \quad , \tag{3.3}$$

where 3 is the number of colors, e_i are the charges of the quarks and the sum runs over the flavors. The fact that $R^{e^+e^-}$ approaches a constant value is a consequence of the lack of renormalization of the conserved electromagnetic current. For finite values of Q^2 there are calculable asymptotic freedom corrections to Eq. (3.3) and the formula for $R^{e^+e^-}$ reads as follows

$$R^{e^+e^-} = R_\infty^{e^+e^-} \left[1 + \frac{\alpha(Q^2)}{\pi} + r^{e^+e^-} \frac{\alpha^2(Q^2)}{\pi^2} \right] \quad , \tag{3.4}$$

where the terms of $O(\alpha^3)$ have been neglected.

The $O(\alpha)$ correction has been calculated in ref.[74].

The coefficient $r^{e^+e^-}$ depends on the definition of α and is given for four flavors as follows [75,76]

$$r^{e^+e^-} = \begin{cases} 1.52 & \overline{MS} \\ -1.70 & MOM \end{cases} . \qquad (3.5)$$

Inserting our standard values of α at $Q^2=30\ GeV^2$, i.e., $\alpha_{\overline{MS}}=0.20$ and $\alpha_{MOM}=0.25$ we obtain the following results for the square bracket in Eq. (3.5)

$$[\overline{MS}] = 1 + 0.064 + 0.006 = 1.070$$
$$[MOM] = 1 + 0.080 - 0.011 = 1.069 \qquad (3.6)$$

We observe that

a) $O(\alpha)$ and $O(\alpha^2)$ corrections to $R^{e^+e^-}$ are small in both schemes,

b) the two schemes in question lead to the same final result for $R^{e^+e^-}$.

A careful comparison of Eq. (3.4) with experimental data involves smearing over the resonances and inclusion of threshold effects. We refer the interested reader to ref. [77] for details. A recent analysis of this type has been done by Barnett, et al. [78], who find that the data are 15% above the theory predictions. Since the data have a systematic error O(10%) this finding is not too disturbing.

One may however, speculate that this "discrepancy" between theory and experiment is due to production of some new objects. Such speculations and references to further literature can be found in ref.[78].

3.2 Photon Structure Functions

The process $\gamma+\gamma\rightarrow$hadrons can be measured in $e^+e^-\rightarrow e^+e^-+$hadrons as shown in Fig. 11. When one photon has large Q^2 and the other is close to its mass-shell the photon-photon process can be viewed as deep-inelastic scattering on a photon target. The corresponding virtual Compton amplitude is shown in Fig. 12 and as in the standard deep-inelastic scattering one can introduce structure functions as F_2^γ, this time photon structure functions.

As depicted in Fig. 12 there are two contributions to the process in question. One in which the target photon behaves as a hadron (Fig.12a) and another one in which the photon acts as a point-like particle (Fig.12b). This separation into two components can be elegantly expressed as follows [79]

$$F_{2,n}^\gamma \equiv \int_0^1 dx\ x^{n-2} F_2^\gamma(x,Q^2) \tag{3.7}$$

$$= \sum_{i=NS,S,G} C_{2,n}^i \langle\gamma|O_i^n|\gamma\rangle + C_{2,n}^\gamma \langle\gamma|O_\gamma^n|\gamma\rangle \quad . \tag{3.8}$$

The sum in Eq.(3.8) represents the first contribution above with operators and coefficient functions identical to those encountered in the standard deep-inelastic scattering (see Eq.(2.2)). The matrix elements $\langle\gamma|O_i^n|\gamma\rangle$ are for i=NS,S,G incalculable in perturbation theory but can be estimated in the vector dominance model. The coefficient functions $C_{2,n}^i$(i=NS,S,G) are already known from Section 2 (Recall that the coefficient functions do not depend on the target). Therefore this component will be for n>2 suppressed by power of log Q^2. For n=2 it contributes a constant term due to the vanishing of the anomalous dimension d_2^- of Eq.(2.10').

The last term on the r.h.s. of Eq.(3.8) represents the point-like contribution. The operator O_γ^n which is not present in the analysis of the deep-inelastic scattering off hadronic targets, is the analog of the gluon operator O_G^n. As noted by Witten, [79], O_γ^n must be included in the analysis of photon-photon scattering. The reason is that, although the Wilson coefficients C_n^γ are $O(\alpha_{EM})$, the matrix elements $\langle\gamma|O_\gamma^n|\gamma\rangle$ are O(1). Therefore the photon contribution in Eq.(3.8) is of the same order in α_{EM} as the contributions of quark and gluon operators. The latter have Wilson coefficients O(1) but matrix elements in photon states $O(\alpha_{EM})$.

What is interesting about the point-like contribution of Eq.(3.8) is that it can not only be calculated in Perturbative QCD but it also dominates at large Q^2. One

obtains

$$F_{2,n}^{\gamma}(Q^2) = \alpha_{EM}^2 \frac{a_n}{\beta_0}\left[\frac{\alpha(Q^2)}{4\pi}\right]^{-1}\left[1-R_n^{\gamma}\frac{\alpha(Q^2)}{4\pi}\right] \tag{3.9}$$

$$= \alpha_{EM}^2[a_n \ln\frac{Q^2}{\Lambda^2} + \tilde{a}_n \ln\ln\frac{Q^2}{\Lambda^2} + b_n] \quad , \tag{3.10}$$

where terms which vanish for $Q^2\to\infty$ have been neglected.

The constants a_n have been calculated by Witten [79]. The parameters

$$R_n^{\gamma} = -\frac{b_n}{a_n}\beta_0 \quad , \tag{3.11}$$

which depend on the definition of α, have been calculated in ref.[80], and are compared to the analogous parameters of the standard deep-inelastic scattering (Eq. 2.10) in Fig. 13.

We observe that the next to leading order corrections to photon structure function F_2^{γ} are in the $\overline{MS}$ and MOM schemes slightly larger than the corresponding corrections to the hadronic deep inelastic structure function F_2^{NS} of Section 2. We do not show in Fig. 13 the prameter R_2^{γ} which involves the perturbatively uncalculable photon matrix element of the hadronic energy momentum tensor, for which $\bar{d}_2=0$ (see the comment above). Recently the calculation of ref.[80] has been confirmed by Duke and Owens [81]. The moments $F_{2,n}^{\gamma}(Q^2)$ are shown in Fig. 14 for $Q^2=10$ GeV^2, and for our standard

values of $\Lambda_{\overline{MS}}$ and Λ_{MOM}. We observe that the $\overline{MS}$ and MOM schemes lead to the same final prediction for $F_{2,n}^{\gamma}$. For comparison the leading order prediction, that of Witten, is also shown in Fig. 14. The moments of Eq. (3.9) can be inverted to give $F_2^{\gamma}(x,Q^2)$, which is shown in Fig. 15. Also the leading order predictions are shown there. We observe that whereas for $0.3 \leq x \leq 0.8$ the next to leading order corrections are small, they are large for small and very large values of x. For small x we expect however vector dominance contributions to be important. For very large x the large corrections can probably be handled as discussed in Section 4. In any case the absolute prediction for F_2^{γ} in the range $0.3<x<0.8$ should be amenable to experimental tests. In this range of x the vector dominance contribution, which decreases with increasing x is relatively small already for $Q^2=10$ GeV^2, and in addition as we have seen above the perturbative expansion in α seems to behave well. Experimentalists should therefore find F_2^{γ} to be an increasing function of x up to $x\approx 0.7$ and a decreasing function of x for $x>0.7$. The last feature is a particular prediction of QCD, which is not present in the simple parton model (the second diagram in Fig. 12 without gluon corrections). In the latter

$$F_n^{\gamma}(x,Q^2) \sim [x^2+(1-x)^2] \ln Q^2 \quad ,$$

i.e., $F_2^{\gamma}(x,Q^2)$ is a monotonically increasing function of x.

Preliminary measurements of $F_2^\gamma(x,Q^2)$ [82] indicate that for intermediate values of x the increase of the photon structure function with increasing x is seen. Large errorbars for larger values of x make it as yet impossible to test the turnover as predicted by QCD. In any case these data indicate that the point-like contribution dominates over the vector dominance contribution already at present values of Q^2. Recall that the vector dominance photon structure function decreases with increasing x.

The formal discussion of photon structure functions presented here can be put on a more intuitive level, in which case the quark and gluon distributions in a photon are the basic elements. The presentation of this intuitive approach can be found in ref.[83]. Further aspects of photon structure functions are discussed in ref.[84,85]. In particular Hill and Ross [85] discuss heavy quark mass effects in photon-photon scattering which turn out to be important. Of interest is also the paper by Chase [86], where the scattering of two far off-shell photons (large p^2 and large Q^2 in Fig. 11) is considered.

Finally the polarized photon structure functions are discussed in ref.[87].

3.3 Paraquarkonium Decays

We begin our discussion of heavy quarkonium decays with the paraquarkonium ($^1S_0$) decays. Consider the ratio

$$P \equiv \frac{9e_Q^4\alpha_{EM}^2}{2} \frac{\Gamma(^1S_0 \to \text{hadrons})}{\Gamma(^1S_0 \to \gamma\gamma)} \tag{3.12}$$

where α_{EM} is the electromagnetic coupling constant and e_Q is the charge of the constituent quark. As discussed in ref.[88], and recently more generally in ref.[89], the ratio P should be insensitve to bound state effects and should be calculable in perturbation theory in $\alpha(Q^2)$. In the leading order we have [90]

$$P_{LO} = [\alpha_{LO}(Q^2)]^2 = \left[\frac{12\pi}{25\ln(Q^2/\Lambda_{LO}^2)}\right]^2 , \tag{3.13}$$

where the numerical factors correspond to four effective flavors. What the relevant value of Q^2 is, will be discussed below.

If next to leading order corrections are taken into account we obtain

$$P = [\alpha_i(Q^2)]^2 [1+H_i(r) \frac{\alpha_i(Q^2)}{\pi}] \tag{3.14}$$

$$= \left[\frac{12\pi}{25\ln(Q^2/\Lambda_i^2)}\right]^2 \left[1+0.48 \frac{\bar{H}_i(r,Q^2)}{\ln(Q^2/\Lambda_i^2)}\right] , \tag{3.15}$$

where

$$\bar{H}_i(r,Q^2) = H_i(r) - 3.08\ \ln\ln\left(\frac{Q^2}{\Lambda_i^2}\right) \quad , \tag{3.16}$$

and in obtaining (3.15), Eq.(2.9) has been used. The index i in Eqs. (3.14)-(3.16) distinguishes between various definitions of the effective coupling constant. The index r distinguishes between various choices of Q^2. Let us take

$$Q^2 = [rm]^2 \quad , \tag{3.17}$$

with m being the mass of the contituent quark. Then we have the relation

$$H_i(r_1) = H_i(r_2) + 8.33\ \ln\left(\frac{r_1}{r_2}\right) \quad . \tag{3.18}$$

In particular

$$H_i(1) = H_i(2) - 5.77 \quad . \tag{3.19}$$

The parameters $H_i(2)$ have been calculated in ref.[88] in t'Hooft's MS scheme. Using the corresponding values for $\overline{MS}$ and MOM schemes [28,91], together with Eqs. (3.16) an (3.19) we can construct the Table III.

We note that

a) H_i and $\bar{H}_i$ are sensitive to the choice of the scheme for α and to the parameter r[91].

b) the two-loop contributions to the β function have an important effect [28]. In the absence of these two-loop effects $H_i=\bar{H}_i$. These properties are due to the fact that the perturbative expansion for the ratio P begins in α^2. In deep-inelastic scattering where the perturbative expansion for the relevant moments of structure functions begins with $[\alpha(Q^2)]^k (k\leq 1)$ the effects a) and b) are much weaker.

Two remarks in connection with the properties a) and b) should be made. First if perturbative expansion for P is behaving well it is <u>irrelevant</u> what we take for r or i, since the differences in H_i or $\bar{H}_i$ due to the change of these parameters will be compensated by the corresponding differences in the value of the effective coupling constant. Thus eventually a unique (up to still higher order corrections not included in the analysis) value for P should be obtained. We shall check below by using our standard values of $\alpha_{\overline{MS}}$ and α_{MOM} whether this is indeed the case.

Second one may wonder why we worry about the two-loop β contributions at all. After all, in contrast to deep-inelastic scattering, we do not study here the evolution of the effective coupling constant. The point is however, that since the ratio P, in contrast to deep-inelastic structure functions, is completely calculable in perturbative QCD, we are interested in the numerical values of α. As we

have discussed in Section 2 (see Fig. 4), these values in $\overline{MS}$ and MOM schemes are substantially suppressed by two-loop β effects (see Eq. 2.9) relatively to the leading order coupling constant. Therefore the two-loop contributions in question are a relatively important part of the next to leading order corrections to quarkonium decays and should be included in the analysis either implicitly as in Eq.(3.14) or explicitly as in Eq.(3.15).

In Table IV we give the values of the second square brackets in Eqs. (3.14) and (3.15) for our standard Λ_i, the cases of Table III, and m=5 GeV, i.e., paraquarkonium in the T family. In the leading order all the entries in Table IV would be equal to unity. We observe that if Q=2m the next to leading order corrections in both schemes for α are very large and perturbative expansion in $\alpha(2m)$ cannot be trusted. On the other hand, the next to leading order corrections are smaller if the expansion in the inverse powers of logarithms is made [28]. If Q=m the next to leading order corrections in the MOM scheme and $\overline{MS}$ scheme are small for the α expansion and $[\log]^{-1}$ expansion respectively.

More generally it has been argued in refs.[30] and [91] that the choice Q=m should lead to a fast convergence of the perturbative series for P.

In spite of the fact that the numerical values in Table IV are very different for different cases, the final results for the ratio P are within 20-30% the same, as shown in Table V. Thus our rough estimate, based on Λ_i of Eq.(2.17), is

$$P = (6.8 \pm 1.6) \cdot 10^{-2} \quad . \tag{3.20}$$

We do not think one can do much more accurate estimate of P without performing still higher order calculations. Except that maybe the method of ref.[31] could decrease the uncertainty in Eq.(3.20), but we have not studied this question.

There is an important lesson to be drawn from this section. We have seen that the $\overline{MS}$ and MOM schemes lead to essentially the same QCD predictions for deep-inelastic scattering, $R^{e^+e^-}$ and photon structure functions. The same results would also be obtained in any other scheme for which the scale parameter $\tilde{\Lambda}$ satisfies $\Lambda_{\overline{MS}} \leq \tilde{\Lambda} \leq \Lambda_{MOM}$. On the other hand we have found [28,30,91] that if only two terms in the perturbative expansion for P are retained, the final answer for P shows a non-negligible sensitivity to the definition of α (see Table V). This is due to the fact that the perturbative expansion for P begins with α^2. We expect that the same feature will be found in the case of quantities for which the perturbative expansions begin with high powers of α, such as many exclusive cross-sections, branching ratios for orthoquarkonium decays and large $p_\perp$ cross-sections. For these quantities also the two-loop contributions to the β function will have generally an important effect.

3.4 Other Quarkonia Decays

So far we have only discussed next-to-leading order corrections to the S-wave $J^{PC}=0^{-+}$ quarkonium decays. Recently similar calculations have been done for P-wave quarkonia decays [92]. We just list the results. Taking r=1 and MOM scheme one obtains (for T family)

$$P(0^{++}) = \alpha^2[1 + 3.9\,\frac{\alpha}{\pi}] \tag{3.21}$$

$$P(2^{++}) = \alpha^2[1 - 0.1\,\frac{\alpha}{\pi}] \tag{3.22}$$

to be compared to (see Table III)

$$P \equiv P(0^{-+}) = \alpha^2[1 + 1.8\,\frac{\alpha}{\pi}] \quad . \tag{3.23}$$

Further recent discussions of higher order corrections to quarkonia decays can be found in refs.[92] and [93]. General discussion of quarkonium physics and references to older papers can be found in [94] and in Section 7.5 of ref.[5].

4. Review of Higher Order Corrections II

In this section we discuss the higher order corrections to various semi-inclusive cross-sections for which the factorization shown in Eq.(1.1) has to be made. After some general remarks concerning infrared divergences, and mass singularities (Section 4.1), we recall in Section 4.2 the basic structure of QCD formulae for semi-inclusive processes. In Section 4.3 we present a procedure for a proper extraction of various elements of these formulae from perturbation theory. Section 4.4 is devoted to fragmentation functions. In Section 4.5 we discuss and compare the higher order QCD corrections to the following processes

$$\begin{aligned} &\text{i)} \quad eh \to eX \\ &\text{ii)} \quad e^+e^- \to hX \\ &\text{iii)} \quad h_1h_2 \to \mu^+\mu^-X \\ &\text{iv)} \quad eh_1 \to eh_2X \\ &\text{v)} \quad e^+e^- \to h_1h_2X \end{aligned} \tag{4.1}$$

where X stands for anything.

Regularities in these corrections are emphasized. In some of these processes the higher order corrections turn out to be large due to the appearance of so called π^2 - and $(\ln n)^2$ terms. Methods of dealing with these terms are briefly

reviewed in Section 4.6. Finally in Section 4.7 we list and briefly discuss the remaining higher order QCD calculations done so far in the literature.

4.1 Infrared Divergences and Mass Singularities

In doing perturbative calculations in QCD one encounters infrared divergences and mass singularities.

Infrared Divergences [95,96] arise from the presence of soft, real or virtual, massless particles. For instance each of the diagrams of Fig. 16 contains infrared divergence due to the emission of a soft real (Fig. 16a) or virtual (Fig. 16b) (massless) gluon. There is a theorem due to Block and Norsdieck [95,96] which states that in inclusive cross-sections all infrared divergences cancel. This cancellation occurs between diagrams with real and virtual soft gluon emissions. Thus cross-sections which do not discriminate between initial and final states differing by the inclusion of one or more soft gluons are infrared finite. In fact since in any experiment the energy resolution is not perfect all measurable cross-sections satisfy the above criterion and are infrared finite. In particular this is the case of quantities in Eqs. (1.2) and (1.3) (See however Section 4.7).

Mass Singularities (collinear divergences) arise from the presence of coupled massless particles which are moving parallel to each other. For instance emission of a collinear

(massless) gluon by a massless quark leads to a mass singularity. There is a theorem due to Kinoshita [97] and Lee and Nauenberg [98] (KLN theorem) which states that for inclusive enough cross-sections all mass singularities cancel. Thus cross-sections which do not discriminate between initial and final states differing by the replacement of one quark by a quark and one or more collinear gluons are free of mass singularities. A nice example of a cross-section free of mass-singularities is the famous two jet cross-section of Sterman and Weinberg [99], where all collinear gluons and quarks reside in a cone of opening angle $\delta>0$. On the other hand in deep-inelastic scattering the mass singularities remain in the final perturbative cross-section. They are due to the emissions collinear to the incoming particle. This is also the case of cross-sections with individual hadrons (not jets) detected in the final state. Thus all perturbative cross-sections for processes listed in (4.1) contain mass singularities. In order to obtain a finite prediction one has to factor out these mass singularities and absorb them in the wave functions of initial or final hadrons (represented by A_n in Eq. (2.1)), which are incalculable by present methods. This is so called factorization of mass-singularities. The remaining cross-section is free of mass singularities but contains large logarithms ($\log Q^2$) which have to be resummed to all orders in the renormalized coupling constant g^2. To this end one can either use formal methods of renormalization group or other

techniques like summation of ladders. When all orders in g^2 are summed and in each order only leading logarithms are kept, then the leading order corrections of asymptotic freedom discussed in Section 2 are obtained. Summing next-to-leading logarithms to all orders in g^2, one obtains the next-to-leading order corrections of Section 2, and so on.

There are many papers in the literature, which deal with the questions of infrared divergences, mass-singularities and factorization. Some of them can be found in refs.[95-120]. Others are listed in various reviews [2-12]. We shall now present the outcome of these studies in a form useful for phenomenological applications.

4.2 Basic Structure

In perturbative QCD the formulae for the processes listed in Eq. (4.1) have the following general structure:

a)
$$\sigma_h = \sum_i f_i^h(x,Q^2) \otimes \sigma_i(x,\alpha(Q^2)) \qquad (4.2)$$

for the processes i) and ii), and

b)
$$\sigma_{h_1 h_2} = \sum_{ij} f_i^{h_1}(x_1,Q^2) \otimes \sigma_{ij}(x_1,x_2,\alpha(Q^2)) \otimes f_j^{h_2}(x_2,Q^2) \qquad (4.3)$$

for the processes iii) - v).

In the above equations $f_i^h(x,Q^2)$ stand either for the parton distributions (quark, antiquark, gluon) which measure the probability for finding a parton of type i in a hadron h

with the momentum fraction x, or they stand for the fragmentation functions, which measure the probability for a parton of type i to decay into a hadron h carrying the fraction x of the parton momentum. σ_{ij} are the relevant parton cross-section and the summation in Eqs.(4.2) and (4.3) is over quarks, antiquarks and gluons. The $\otimes$ denotes symbolically a convolution, example of which can be found in Eq.(2.46). Equations (4.2) and (4.3) are schematically represented in Figs. 10 and 17, where the circles stand either for parton distributions or parton fragmentation functions, the squares denote parton cross-sections, and the connecting internal lines stand for partons.

The following properties of Eqs.(4.2) and (4.3) should be kept in mind.

1) The Q^2 evolution of parton distributions and parton fragmentation functions is governed by certain equations. In the leading order these are the known Altarelli-Parisi-DDT [50,4] equations. They are the same for parton distributions and parton fragmentation functions [121] except for the transposition of the anomalous dimension matrix. Beyond the leading order three things happen. First, the evolution equations become modified by calculable corrections. Second, this modification is generally different for parton distributions and parton fragmentation functions. Third, the calculable corrections to leading order evolution equations depend on the definition of parton distributions and parton fragmentation functions.

2) The parton cross-sections are calculable in perturbative QCD. For processes i) - v) they are trivial in the leading order and identical to those encountered in the simple parton model. In particular the cross-sections involving gluons are zero. Beyond the leading order three things happen. First, the parton cross-sections involving quarks and antiquarks become modified by calculable corrections. Second, the parton cross-sections involving gluons become non-zero. They are $O(\alpha)$. Third, the order α corrections to all parton cross-sections depend on the definition of parton distributions and parton fragmentation functions.

3) The definition dependences of parton distributions, parton fragmentation functions and of parton cross-sections cancel in the final formulae for σ_h and $\sigma_{h_1 h_2}$ if a consistent calculation of all these quantities is made. In particular for the full cancellation of the definition dependence to occur, all singlet contributions to σ_h and $\sigma_{h_1 h_2}$ have to be included in the analysis [122]. See Section 2.5.2 for a particular example.

4) We have seen in Section II, that an important role in the discussion of deep-inelastic structure functions has been played by the matrix elements of local operators, $A_n(\mu^2)$. In particular, when normalized at $\mu^2=Q^2$, this matrix elements served to define Q^2 dependent parton distributions (see Eqs. 2.33 and 2.43). An analogous role in the case of fragmentation functions is played by so-called time-like cut

vertices introduced by Mueller, [112] which we shall denote by $[V_n(\mu^2)]_T$ with "T" standing for time-like. It can be shown that $A_n(\mu^2)$'s are equivalent to so-called space-like cut vertices [112]. In order to keep a uniform notation we shall denote $A_n(\mu^2)$'s by $[V_n(\mu^2)]_S$ with "S" standing for space-like. Detailed discussion of cut vertices can be found in refs.[112-118]. Here it suffices to say that they are universal (process independent) factors which contain all mass-singularities of the theory. The anomalous dimensions of space-like and time-like cut vertices will be denoted by $[\gamma_n]_S$ and $[\gamma_n]_T$ respectively. The former ones are just the anomalous dimensions of Eq.(2.7).

4.3 Procedure for Calculations

Essentially any experiment, which is relevant for the tests of QCD involves hadrons. On the other hand any perturbative QCD calculation deals with quarks and gluons instead of hadrons. Therefore any perturbative QCD practitioner is faced with the problem of extracting from her (his) perturbative calculation certain elements which can be inserted in the general formulae (4.2) and (4.3). Subsequently Eqs.(4.2) and (4.3) can be directly compared with experimental data. We shall outline here a procedure which accomplishes this program.

Step 1. Calculate the cross-section for a given parton subprocess. For instance in the case of $q\bar{q}$ annihilation contributing to process iii) one has to consider diagrams of

Fig. 18. The result contains mass-singularities (see Section 4.1) which can be regulated by keeping the mass-less quarks and antiquarks at space-like momenta p_1^2, $p_2^2<0$. One obtains for the moments (in $\tau=Q^2/S$) of this cross-section the following expression

$$F_n\left(\frac{Q^2}{p_i^2},g^2\right) = 1 + \frac{g^2}{16\pi^2}\left[-\frac{1}{2}\gamma_{NS}^{o,n}\ln\frac{Q^2}{-p_1^2}-\frac{1}{2}\gamma_{NS}^{0,n}\ln\frac{Q^2}{-p_1^2} + r_n\right] \quad (4.4)$$

where r_n's are independent of Q^2 and p_i^2, and $\gamma_{NS}^{0,n}$ have been defined in Eq.(2.7). The result (4.4) has two bad features

i) it is singular for $p_i^2\to 0$ (mass singularities)

ii) the constants r_n <u>depend on regularization scheme</u> used.

There are two ways to solve these two problems. We begin with the presentation of one of them.

<u>Step 2.</u> Calculate the matrix elements of local operators (or cut vertices) taken between quark states. Such matrix elements contrary to the hadronic matrix elements can be calculated in perturbation theory. Using <u>the same</u> regularization procedure as in the Step 1 one obtains

$$A_n^{(i)}\left(\frac{p_i^2}{\mu^2}.g^2\right) = 1 + \frac{g^2}{16\pi^2}\,\frac{1}{2}\gamma_{NS}^{o,n}\ln\frac{-p_i^2}{\mu^2} + a_n \quad . \quad (4.5)$$

The matrix elements in question are divergent and have to be renormalized. Therefore the appearance of the subtraction point μ^2. The constant terms a_n depend on both regularization scheme and renormalization scheme used. The regularization scheme dependence of a_n is however precisely the same as the one of r_n's in (4.4).

Step 3. Rewrite $F_n(Q^2/p_i^2,g^2)$ of Eq.(4.4) as follows

$$F_n\left(\frac{Q^2}{p_i^2},g^2\right) = \tilde{F}_n\left(\frac{Q^2}{\mu^2},g^2\right) A_n^{(1)}\left(\frac{p_1^2}{\mu^2},g^2\right) A_n^{(2)}\left(\frac{p_2^2}{\mu^2},g^2\right) \quad . \tag{4.6}$$

The function $\tilde{F}_n(Q^2/\mu^2,g^2)$ is free of mass singularities and is given as follows

$$\tilde{F}_n\left(\frac{Q^2}{\mu^2},g^2\right) = 1 + \frac{g^2}{16\pi^2}\left[-\frac{1}{2}\gamma_{NS}^{o,n}\ln\frac{Q^2}{\mu^2} - \frac{1}{2}\gamma_{NS}^{o,n}\ln\frac{Q^2}{\mu^2} + u_n\right] \tag{4.7}$$

with

$$u_n = r_n - 2a_n \quad . \tag{4.8}$$

The constants u_n are regularization scheme independent but depend (through a_n) on renormalization scheme used in the Step 2. Equation (4.6) expresses the factorization of mass singularities which can be proven to all orders in g^2 [108-110]. $\tilde{F}_n(Q^2/\mu^2,g^2)$ is an analog of the coefficient

function $C_{k,n}(Q^2/\mu^2, g^2)$ of Eq. (2.2).

Step 4. The moments of the parton cross-sections of Eqs.(4.3) and (4.4) can now be obtained from $\tilde{F}_n(Q^2/\mu^2, g^2)$ by putting $Q^2=\mu^2$. Denoting these moments by σ_n we have

$$\sigma_n \equiv \tilde{F}_n(1, \bar{g}^2) \quad , \tag{4.9}$$

i.e.,

$$\sigma_n = 1 + \frac{\bar{g}^2}{16\pi^2} u_n \quad . \tag{4.10}$$

This is just the analog of Eq.(2.34). Note that σ_n, which we called in this review "parton cross-section" differs from F_n of Eq.(4.4), which is the true parton cross-section obtained directly from the diagrams of Fig.18. Therefore sometimes in the lierature σ_n is called the "short distance function."

Step 5. For the Q^2 evolution of parton distributions (or fragmentation functions, see Section 4.4), use the evolution equations of Section 2.5 corresponding to the definition A. Care must be taken that the two-loop anomalous dimensions $[\gamma^{(1),n}]_T$ and $[\gamma^{(1),n}]_S$, which enter these evolution equations are calculated in the same renormalization scheme as parameters a_n of Eq.(4.5).

Step 6. Insert results of Steps 4 and 5 into Eqs. (4.2) or (4.3).

This procedure is necessary in order to calculate QCD predictions for processes i) and ii) of Eq.(4.1). However if definition B of parton distributions (see Section 2.5) and an analogous definition of fragmentation function (see Section 4.4) are used, the calculation for processes iii) - v) can proceed as follows. The modifications are in Steps 2, 3, 4 and 5.

Step 2'. In the example above repeat the Step 1 for deep-inelastic scattering using the same regularization scheme as in Step 1. The result is as follows

$$F_n^{DIS}\left(\frac{Q^2}{p_i^2},g^2\right) = 1 + \frac{g^2}{16\pi^2}\left[-\frac{1}{2}\gamma_{NS}^{0,n}\ln\frac{Q^2}{-p_i^2} + r_n^{DIS}\right] \quad i=1,2 \tag{4.11}$$

where r_n^{DIS} are specific to a given regularization scheme. They are however contrary to a_n's in Eq.(4.5) renormalization prescription independent.

Steps 3'. and 4'. The moments of the parton cross-sections, which we now denote by σ_n' can be found from

$$F_n\left(\frac{Q^2}{p_i},g^2\right) = \sigma_n' F_n^{DIS}\left(\frac{Q^2}{p_i},g^2\right)\cdot F_n^{DIS}\left(\frac{Q^2}{p_2},g^2\right) \quad , \tag{4.12}$$

i.e.,

$$\sigma_n' = 1 + \frac{\bar{g}^2}{16\pi^2}u_n' \quad , \tag{4.13}$$

with

$$u_n' = r_n - 2r_n^{DIS} \quad . \tag{4.14}$$

u_n' are regularization and renormalization prescription independent, and are generally different from u_n of Eq. (4.8).

Step 5'. For the Q^2 evolution of parton distributions (or fragmentation functions, see Section 4.4), use the evolution equations of Section 2.5 corresponding to the definition B. Equivalently if QCD agrees well with the experimental data for processes i) and ii) in (4.1), one can use directly the experimental data for the processes in question instead of evolution equations of Section 2.

This completes the presentation of the procedure which should be used together with Eqs.(4.2) and (4.3). One remark is however necessary before we leave this subject. We have stated above that the parameters u_n and u_n' are independent of the regularization scheme used. In fact it has been found in the literature that for the processes which involve more than one (detected and/or target) hadron (processes iii)-v) in (4.1)) u_n and u_n' calculated in the standard off-shell regularization scheme differ from those obtained in the on-shell or dimensional regularization schemes. The discussion is too technical to be presented here, and the reader is referred to the papers of refs.[123-126] for

details. The outcome of these analyses (in particular [123]-[125]) is that whereas in the case of on-shell regularization scheme the procedure above can be directly applied (with $-p_i^2 \to m_i^2, m_i$ being the quark mass), the standard off-shell regularization scheme requires some modifications. Eventually a regularization prescripion independent answer for u_n and u_n' is obtained.

The explicit applications of the first procedure to processes i), ii), iii) and iv) can be found in refs. [22], [125], [127] and [125,128] respectively. Applications of the second procedure can be found in refs. [37,48,129-133].

Needless to say both procedures lead to the same results for the cross-sections σ_h and $\sigma_{h_1 h_2}$ in Eqs. (4.2) and (4.3) respectively.

4.4 Fragmentation Functions and $e^+e^- \to hx$

In Section 2.5 we have discussed parton distributions beyond the leading order. Here we shall present an analogous discussion for fragmentation functions. Subsequently we shall compare the next to leading order corrections to the Q^2 evolution of fragmentation functions with the corresponding corrections for parton distributions. Also a comparison of the full next to leading order corrections for $eh \to eX$ and $e^+e^- \to hX$ in the non-singlet sector will be given.

4.4.1 Corrections to Gribov-Lipatov Relation. We begin by discussing the anomalous dimensions $[\gamma_{NS}^n]_T$ relevant for fragmentation functions and their relation to the anomalous

dimensions $[\gamma_{NS}^n]_S$ which are relevant for parton distributions. The latter anomalous dimensions have been denoted in Section 2 by γ_{NS}^n. $[\gamma_{NS}^n]_S$ and $[\gamma_{NS}^n]_T$ have the following perturbative expansions

$$[\gamma_{NS}^n]_{S,T} = [\gamma_{NS}^{(0),n}]_{S,T} \frac{g^2}{16\pi^2} + [\gamma_{NS}^{(1),n}]_{S,T} [\frac{g^2}{16\pi^2}]^2 + \ldots \tag{4.15}$$

The coefficients $[\gamma_{NS}^{o,n}]_{S,T}$ satisfy the following relation

$$[\gamma_{NS}^{o,n}]_S = [\gamma_{NS}^{o,n}]_T \quad , \tag{4.16}$$

which is due to Gribov and Lipatov [134]. Beyond the leading order this relation is no longer true and we have generally

$$[\gamma_{NS}^{(1),n}]_S = [\gamma_{NS}^{(1),n}]_T + \Delta_n \quad , \tag{4.17}$$

where Δ_n measures the violation of Gribov-Lipatov relation. Since $[\gamma_{NS}^{(1),n}]_{S,T}$ are renormalization prescription dependent, so are Δ_n's and in principle it is possible to find a scheme in which Δ_n=0 [135]. The first calculation of $[\gamma_{NS}^{(1),n}]_T$ has been done by Curci, Furmanski and Petronzio [18]. Recently $[\gamma_{NS}^{(1),n}]_T$ has been calculated in refs.[136] and [137]. The

results of these three groups are compatible with each other, although numerical values for $[\gamma_{NS}^{(1),n}]_T$ differ due to different conventions used in these papers. We shall present here the results of ref.[18].

The values of $[\gamma_{NS}^{(1),n}]_S$ and $[\gamma_{NS}^{(1),n}]_T$ obtained in $\overline{MS}$ scheme [22] in ref.[17] and ref.[18] respectively are given in Table VI. Also the values of the parameters

$$[Z_n^{NS}]_{S,T} = \frac{[\gamma_{NS}^{(1),n}]_{S,T}}{2\beta_0} - \frac{\gamma_{NS}^{(0),n}}{2\beta_0^2}\,\beta_1 \tag{4.18}$$

are shown there. Note that Δ_n vanishes for n going to infinity.

4.4.2 Definition A. Now consider the evolution equations of parton distributions and parton fragmentation functions corresponding to the definition A of Section 2.5. We have

$$\langle q^{NS}(Q^2)\rangle_n^{(a)} = \langle q_0^{NS}(Q^2)\rangle_n^{(a)} \left[\frac{\alpha(Q^2)}{\alpha(Q_0^2)}\right]^{d_n^{NS}} \left[1+[Z_n^{NS}]_S \frac{\alpha(Q^2)-\alpha(Q_0^2)}{4\pi}\right] \tag{4.19}$$

and

$$\langle D^{NS}(Q^2)\rangle_n^{(a)} = \langle D^{NS}(Q_0^2)\rangle_n^{(a)} \left[\frac{\alpha(Q^2)}{\alpha(Q_0^2)}\right]^{d_n^{NS}} \left[1+[Z_n^{NS}]_T \frac{\alpha(Q^2)-\alpha(Q_0^2)}{4\pi}\right] \tag{4.20}$$

Here in analogy with Eq.(2.33)

$$<D^{NS}(Q^2)>_n^{(a)} = \int_0^1 dz\ z^{n-1} D_a^{NS}(z,Q^2) = [V_n^{NS}(Q^2)]_T \qquad (4.21)$$

are the moments of an effective Q^2 dependent non-singlet fragmentation function $D_a^{NS}(z,Q^2)$, and $[V_n^{NS}(Q^2)]_T$ denotes a time-like cut vertex normalized at $\mu^2=Q^2$. Finally z is the fraction of the parton momentum carried by the hadron in the final state.

On the basis of Eqs.(4.19) and (4.20), and the Table VI we conclude that in the case of definition A and in the $\overline{MS}$ scheme [138]

i) evolution equations for parton distributions and parton fragmentation functions are essentially the same, i.e., Gribov-Lipatov relation is effectively violated very weakly,

ii) evolution equations in question are essentially the same as leading order equations except for the modified evolution of the effective coupling constant (see Eq.(2.9)).

4.4.3 Definition B. Here in analogy with Eq. (2.33')

$$<q^{NS}(Q^2)>_n^{(b)} = <q^{NS}(Q_0^2)>_n^{(b)} \left[\frac{\alpha(Q^2)}{\alpha(Q_0^2)}\right]^{d_n^{NS}} \left[1+[R_n^{NS}]_S \frac{\alpha(Q^2)-\alpha(Q_0^2)}{4\pi}\right] \qquad (4.19')$$

and

$$<D^{NS}(Q^2)>_n^{(b)} = <D^{NS}(Q_0^2)>_n^{(b)} \left[\frac{\alpha(Q^2)}{\alpha(Q_0^2)}\right]^{d_n^{NS}} \left[1+[R_n^{NS}]_T \frac{\alpha(Q^2)-\alpha(Q_0^2)}{4\pi}\right] \tag{4.20'}$$

where

$$[R_n^{NS}]_{S,T} = [Z_n^{NS}]_{S,T} + [B_n^{NS}]_{S,T} \quad . \tag{4.22}$$

The $[B_n^{NS}]_S$ and $[B_n^{NS}]_T$ enter the perturbative expansion of the coefficient functions of space-like and time-like cut vertices respectively, i.e.

$$[C_n^{NS}(1,\bar{g}^2]_{S,T} = 1 + [B_n^{NS}]_{S,T} \frac{\bar{g}^2}{16\pi^2} \quad . \tag{4.23}$$

$[C_n^{NS}(1,\bar{g}^2)]_{S,T}$ are "short distance functions" which we called parton cross-sections in the case of definition A (see Eq. 2.34). In the case of definition B they are absorbed into the parton distributions and parton fragmentation functions. We know already $[B_n^{NS}]_S$ from Section 2. $[B_n^{NS}]_T$ can be extracted from $e^+e^-\to hX$ by using the procedure of Section 4.2. One finds [18,125] that $[B_n^{NS}]_T$ and $[B_n^{NS}]_S$ differ considerably from each other at all n, and that the difference is mainly due to the continuation of Q^2 from space-like to time-like region. In particular at large n one finds a simple relation (see also (4.36) and 4.37))

$$[B_n^{NS}]_T = [B_n^{NS}]_S + \frac{8}{3}\pi^2 \quad . \tag{4.24}$$

where $8/3\pi^2$ results from the continuation in question. At small n there are additional differences between $[B_n^{NS}]_T$ and $[B_n]_S$ which are not neglegible. In order to make this discussion more quantitative we have plotted in Fig. 19 the last factor of the following formal expression

$$[M^{NS}(n,Q^2)]_{S,T} = [\tilde{A}_n]_{S,T}[\alpha(Q^2)]^{d_n^{NS}}[1+\frac{\alpha(Q^2)}{4\pi}[R_n^{NS}]_{S,T}] \tag{4.25}$$

which is a generalization of Eq. (2.10). Results for $\overline{MS}$ and MOM schemes are shown for our standard values of Λ_i given in Eq. (2.17). We observe that the next-to-leading order corrections to $e^+e^-\to hx$ are in both $\overline{MS}$ and MOM schemes larger than the corresponding corrections in deep-inelastic scattering.

On the basis of Eqs. (4.19'), (4.20') and Fig. 19 we conclude that in the case of definition B

i) evolution equations for parton distributions and parton fragmentation functions differ at "low" values of $Q^2 \leq 100$ GeV^2 from each other.

ii) evolution equations in question differ substantially at large n (large x) from the corresponding leading order equations due to the large values of $[B_n]_{S,T}$ at large n

$$[B_n^{NS}]_T = [B_n^{NS}]_S + \frac{8}{3}\pi^2 \quad . \tag{4.24}$$

where $8/3\pi^2$ results from the continuation in question. At small n there are additional differences between $[B_n^{NS}]_T$ and $[B_n]_S$ which are not neglegible. In order to make this discussion more quantitative we have plotted in Fig. 19 the last factor of the following formal expression

$$[M^{NS}(n,Q^2)]_{S,T} = [\tilde{A}_n]_{S,T}[\alpha(Q^2)]^{d_n^{NS}}[1+\frac{\alpha(Q^2)}{4\pi}[R_n^{NS}]_{S,T}] \tag{4.25}$$

which is a generalization of Eq. (2.10). Results for $\overline{MS}$ and MOM schemes are shown for our standard values of Λ_i given in Eq. (2.17). We observe that the next-to-leading order corrections to $e^+e^-\to hx$ are in both $\overline{MS}$ and MOM schemes larger than the corresponding corrections in deep-inelastic scattering.

On the basis of Eqs. (4.19'), (4.20') and Fig. 19 we conclude that in the case of definition B

i) evolution equations for parton distributions and parton fragmentation functions differ at "low" values of $Q^2 \leq 100$ GeV^2 from each other.

ii) evolution equations in question differ substantially at large n (large x) from the corresponding leading order equations due to the large values of $[B_n]_{S,T}$ at large n

and due to the non-trivial behavior $(\ln n)^2$ of these parameters (see Section 2.5 and 4.5).

In summary due to the fact that $[R_n^{NS}]_T > [R_n^{NS}]_S$ we expect scaling violations in $e^+e^- \to hX$ to be larger than in $eh \to eX$.

4.5 Higher Order Corrections to Various Semi-Inclusive Processes

We shall here complete our discussion of higher order corrections to the processes shown in Fig.17. We know already the Q^2 evolution of the parton distributions and parton fragmentation functions (Sections 2.5 and 4.3), which are denoted in Fig.17 by circles. We also know the parton cross-sections (the squares in Fig.17) relevant for $eh \to eX$ and $e^+e^- \to hX$. What remains then to discuss are the parton cross-sections for the processes of Fig. c-e, for which the general formula (4.3) applies. There are usually several sub-processes contributing in order $\alpha(Q^2)$, but we shall concentrate here on those which involve only quark (antiquark) distributions and fragmentation functions. First these subprocesses contribute in the leading order. Second in the case of the definitions A and B (Sections 4.3 and 2.5) the dominant part of the next-to-leading order corrections to the processes in Fig. 17 comes from these subprocesses. It is of course possible to define parton densities in such a way that in a large kinematical range the corrections coming from subprocesses involving gluon densities are most important. But then our discussion would be less transparent.

Let us denote the moments of the cross-sections σ_h and σ_i of Eq.(4.2) generally by

$$\sigma_n(Q^2) = \int_0^1 dx\ x^{n-2}\sigma(x,Q^2) \quad , \tag{4.26}$$

and the double moments of the cross-sections $\sigma_{h_1h_2}$ and σ_{ij} of Eq.(4.3) by

$$\sigma_{nm}(Q^2) = \int_0^1 dx_1 \int_0^1 dx_2\ x_1^{n-2}x_2^{m-2}\sigma(x_1,x_2,Q^2) \quad , \tag{4.27}$$

where x, x_1 and x_2 are the relevant scaling variables. Then the moments of the cross-sections for the processes i)-v) of Eq.(4.1) can be written (neglecting obvious overall factors as $4\pi\alpha_{EM}/3Q^2$ in (4.30)) as follows

$$\sigma_n^{DIS}(Q^2) = \langle q(Q^2)\rangle_n^{(a)} \left[1+ \frac{\alpha(Q^2)}{4\pi}\ [B_n]_S\right] \quad , \tag{4.28}$$

$$\sigma_n^{e^+e^-\to hX}(Q^2) = \langle D(Q^2)\rangle_n^{(a)} \left[1+ \frac{\alpha(Q^2)}{4\pi}\ [B_n]_T\right] \quad , \tag{4.29}$$

$$\sigma_{nm}^{DY}(Q^2) = \langle q(Q^2)\rangle_n^{(a)} \langle \bar{q}(Q^2)\rangle_m^{(a)} \left[1+ \frac{\alpha(Q^2)}{4\pi}\ B_{nm}^{DY}\right] \quad , \tag{4.30}$$

$$\sigma_{nm}^{eh_1\to h_2X}(Q^2) = \langle q_{h_1}(Q^2)\rangle_n^{(a)} \} \langle D_{h_1}(Q^2)\rangle_m^{(a)} \left[1+ \frac{\alpha(Q^2)}{4\pi}\ B_{nm}^{eh}\right] \tag{4.31}$$

$$\sigma_{nm}^{e^+e^-\to h_1h_2X}(Q^2) = \langle D_{h_1}(Q^2)\rangle_n^{(a)} \langle D_{h_2}(Q^2)\rangle_m^{(a)} \left[1+ \frac{\alpha(Q^2)}{4\pi} B_{nm}^{e^+e^-}\right] . \tag{4.32}$$

We have used here the definition A of parton densities and we have expanded the parton cross-sections in power of α keeping only the next-to-leading terms. Furthermore to make the formulae more transparent we have not summed over quarks and antiquarks. The parton cross-sections for these additional subprocesses are exactly the same to this order as the parton cross-sections shown in (4.28)-(4.32). The references where the explicit calculations of the parameters B_n and B_{nm} can be found are listed at the end of Section 4.3.

Let us recall that the Q^2 evolution of parton densities so defined is essentially equivalent to the leading order evolution except for the modification of $\alpha(Q^2)$. Therefore the dominant part of the next-to-leading order corrections to the processes in question resides in the parameters B_n and B_{nm}.

It turns out that there are certain regularities in the n and m dependence of the coefficients B_n and B_{nm}[139]. In order to find them it is instructive to calculate the large n and m behavior of these coefficients neglecting only the terms O(1/n,1/m). To this end the following formulae for the large n behavior of various functions which enter B_n and B_{nm} are very useful [23]

$$S_1(n) = \sum_{j=1}^{n} \frac{1}{j} \to \log n + \gamma_E \quad , \tag{4.33}$$

$$S_2(n) = \sum_{j=1}^{n} \frac{1}{j^2} \to \frac{\pi^2}{6} \quad , \tag{4.34}$$

$$G_1(n) = \sum_{j=1}^{n} \frac{1}{j} \sum_{\ell=1}^{j} \frac{1}{\ell} = \frac{1}{2}\{S_1^2(n)+S_2(n)\} \quad . \tag{4.35}$$

Here γ_E=0.5772 is the Euler-Masheroni constant. Using these formulae and the convenient table of Mellin transforms of ref. [48] we have obtained [139] the large n and m behavior of B_n and B_{nm}:

$$[B_n]_S \Rightarrow F_n^{(1)} \quad , \tag{4.36}$$

$$[B_n]_T \Rightarrow F_n^{(1)} + [1]\frac{8}{3}\pi^2 \quad , \tag{4.37}$$

$$B_{nm}^{eh} \Rightarrow F_{nm}^{(2)} + [1]\frac{8}{3}\pi^2 \quad , \tag{4.38}$$

$$B_{nm}^{DY} \Rightarrow F_{nm}^{(2)} + [2]\frac{8}{3}\pi^2 \quad , \tag{4.39}$$

$$B_{nm}^{e^+e^-} \Rightarrow F_{nm}^{(2)} + [2]\frac{8}{3}\pi^2 \quad , \tag{4.40}$$

where the universal functions $F_n^{(1)}$ and $F_{nm}^{(2)}$ are given in the $\overline{MS}$ scheme as follows

$$F_n^{(1)} = \frac{4}{3}\{2(\log n)^2 + (3+4\gamma_E)\log n + 3\gamma_E + 2\gamma_E^2 - 9 - \frac{\pi^2}{3}\} \quad (4.41)$$

$$F_{nm}^{(2)} = \frac{4}{3}\{2(\log n)^2 + 2(\log m)^2 + 4 \log m \log n + 8\gamma_E \log m + 8\gamma_E \log n + 8\gamma_E^2 - 16 - \frac{4}{3}\pi^2\} \quad . \quad (4.42)$$

We are now in the position to list the important properties of the parameters B_n and B_{nm}.

1) For large n and m there is a universality in the n and m dependence of B_n and B_{nm} at the level of $(\log n)^2$, log m log n, log n and constant terms, which is broken only by a process dependent number ([...]) of the $8/3\pi^2$ terms.

2) We have found [139] a simple counting rule for the number of "$8/3\pi^2$" terms one has to add to the universal function for a given process. This "$8/3\pi^2$ counting rule" reads as follows: count the number of target hadrons and/or

hadrons detected in the final state, which are on the other side of the large momentum. This is illustrated in Fig.20.

3) As shown in Fig.19, at low n the universal behavior of $[B_n]_S$ and $[B_n]_T$ is no longer satisfied. We have found however that the exact values of B^{eh}_{nm}, B^{DY}_{nm} and $B^{e^+e^-}_{nm}$ for $m,n \geq 6$ are all equal to each other (except for $8/3\pi^2$ terms) within 5%. For m=4 and n=6 or vice versa the equality in question is within 10-15%. We have no simple explanation for this approximate universality at relatively low n and m values.

4) In Fig.21 we have shown B^{DY}_{nm} for n=m. We observe that due to the term [2] $8/3\pi^2$ the corrections are large at all values of n and m, although they are substantially smaller in MOM scheme than in $\overline{MS}$ scheme. With increasing n and/or m B^{DY}_{nm} increase fast due to $(\log n)^2$ or $\log n \log m$ terms. Similar results are obtained for $B^{e^+e^-}_{nm}$. For B^{eh}_{nm} the corrections are relatively small for small values of n and m but are large for $n,m \geq 6$.

5) The parameters B^{eh}_{nm} and $B^{e^+e^-}_{nm}$ are much smaller if the definition B of parton distributions and parton fragmentation functions is used. In this case B^{eh}_n, $B^{e^+e^-}_{nm}$ and B^{DY}_{nm} are replaced as follows

$$B^{eh}_{nm} \to B^{eh}_{nm} - [B_n]_S - [B_m]_T \equiv \tilde{B}^{eh}_{nm} \quad , \tag{4.43}$$

$$B^{e^+e^-}_{nm} \to B^{e^+e^-}_{nm} - [B_n]_T - [B_m]_T = \tilde{B}^{e^+e^-}_{nm} \quad , \tag{4.44}$$

$$B_{nm}^{DY} \to B_{nm}^{DY} - [B_n]_S - [B_m]_S = \tilde{B}_{nm}^{DY} \quad . \tag{4.45}$$

Since the $8/3\pi^2$ terms have been now absorbed in the definition of fragmentation functions $\tilde{B}_{nm}^{eh}$ and $\tilde{B}_{nm}^{e^+e^-}$ are only large for $n,m \geq 8$. For $n,m \geq 6$ they lead to corrections of order 15%. For the massive muon production ($\tilde{B}_{nm}^{DY}$) the corrections are still large at all values of n and m (although smaller than in the case of def.A). Here the $8/3\pi^2$ terms are not cancelled.

6) Due to the terms $\log n \cdot \log m$ the next to leading order corrections introduce non-factorization in n and m [128,125,130,131]. For the semi-inclusive deep-inelastic scattering $eh \to h_2 X$ this corresponds to non-factorization in x and z variables which has been studied in ref.[140].

Some of the implications of these results for phenomenology will be discussed at the end of this section.

4.6 Summing Large Perturbative Corrections in QCD

We have seen in Sections 4.4 and 4.5 that generally the next-to-leading order corrections to semi-inclusive processes are large at accessible values of Q^2 for which $0.2 \leq \alpha(Q^2) \leq 0.4$. There are two sources of these large corrections:

i) π^2 terms

and

ii) $(\log n)^2$, etc. terms.

Can we do anything about these larger corrections?

4.6.1 Attempts to Redefine α The parameters $[B_n]_S$, $[B_n]_T$ and B_{nm} in Eqs.(4.38)-(4.40) depend on the definition of the effective coupling constant. In particular as shown in Figs.19 the next-to-leading order corrections in the MOM scheme are smaller than in the $\overline{MS}$ scheme. Now any redefinition of the effective coupling constant corresponds to the following changes in the parameters B_n and B_{nm}:

$$B_n \to B_n + b\, d_{NS}^n \quad , \tag{4.46}$$

$$B_{nm} \to B_{nm} + b[d_{NS}^n + d_{NS}^m] \quad , \tag{4.47}$$

where b is a constant and $d_{NS}^n \sim \log n$ at large n.

We may therefore try to find a scheme for which corrections are small for all processes. It is a trivial matter to convince onceself that this is impossible. See Fig.22.

First we find that the terms $[\log n]^2$ and $\log m \cdot \log n$ are not affected by the redefinition of α. This is what we already know from Section 2. Secondly if we choose the parameter b in Eqs. (4.46) and (4.47) to cancel the $8/3\pi^2$ term in $[B_n]_T$ we will spoil the perturbative expansion in deep-inelastic scattering for low values of n, which are the most relevant moments for present phenomenology. The situation is even worse if we try to cancel the terms $8/3\pi^2$

in the Drell-Yan cross-sections. That the redefinition of $\alpha(Q^2)$ cannot make all corrections to be small is also clear from the fact that $\tilde{B}_{nm}$ of Eqs. (4.43)-(4.45), which are independent of the definition of α, are large for large n and m. In the case of Drell-Yan this is also the case for low n,m. We have now a few choices.

Choice 1: Wait until Q^2 is so large that $\alpha(Q^2)$ is small enough to make perturbative expansions reliable. Note that if $\alpha=\alpha_{EM}$ all the corrections discussed here are of order of a few percent.

This is definitely a passive and a pessimistic approach.

Choice 2: We may try to argue that for some processes the effective α (in a given renormalization scheme) should be evaluated at a momentum different from Q^2; e.g., $Q^2(1-x)$. We have seen in Section 3 that in the case of paraquarkonium decays the change of the argument of α considerably improved the perturbative expansion. Since in semi-inclusive processes higher order corrections depend on n or x we should expect the modified argument of α to be x or n dependent.

Choice 3: It has been pointed out that the large corrections discussed above are due to the emission of soft gluons. Therefore there is a hope that one could resum all the large corrections to all orders in α.

As we shall see the choices 2 and 3 are related to each other. It should be kept in mind that these two approaches (choice 2 and 3) go beyond the standard renormalization group approach. We shall now discuss how one can in principle sum the π^2 and $(\ln n)^2$ terms.

4.6.2 Summing π^2 Terms This question has been first considered in connection with the massive muon production, and not for double moments of Eq.(4.30) but for single moments

$$\sigma_n^{DY}(Q^2) = \int d\tau\ \tau^n \frac{d\sigma^{DY}}{dQ^2} \quad . \tag{4.48}$$

Using the definition B for parton densities, the $q\bar{q}$ contribution to $\sigma_n^{DY}(Q^2)$ is given as follows

$$\sigma_n^{q\bar{q}}(Q^2) = \langle q(Q^2)\rangle_n^{(b)} \langle \bar{q}(Q^2)\rangle_n^{(b)} \left[1+ \frac{\alpha(Q^2)}{4\pi} B_n^{q\bar{q}}\right] \quad . \tag{4.49}$$

$B_n^{q\bar{q}}$ has the following large n behavior

$$B_n^{q\bar{q}} = \frac{4}{3}\{4[\log n]^2 - 1.38 \log n + 13.0\} + \frac{8\pi^2}{3} \ , \tag{4.50}$$

with

$$13.0 = 2\left[2\gamma_E^2 + 1 + \frac{2\pi^2}{3} - 3\gamma_E\right] \quad . \tag{4.51}$$

Note that in Eq. (4.50) the $8\pi^2/3$ and $(\ln n)^2$ are dominant. The appearance of $8\pi^2/3$ term comes from the continuation from space-like (deep-inelastic scattering) to time-like (Drell-Yan) Q^2. It has been suggested [141] that these π^2 contributions can be summed to all orders in $\alpha(Q^2)$ by using the asymptotic formula for elastic quark form factor [142-144]

$$F(q^2) = \exp[-\frac{8}{25}\log(\frac{-q^2}{\Lambda^2})\log[\log(\frac{-q^2}{\Lambda^2})]] \quad . \qquad (4.52)$$

Indeed in the case of the definition B, in which parton densities are defined through deep-inelastic scattering, which involves space-like q^2, $\sigma_n^{q\bar{q}}$ can be written as follows

$$\sigma_n^{q\bar{q}}(Q^2) \cong \langle q(Q^2)\rangle_n^{(b)} \langle \bar{q}(Q^2)\rangle_n^{(b)} |\frac{F(Q^2)}{F(-Q^2)}|^2 \qquad (4.53)$$

$$\cong \langle q(Q^2)\rangle_n^{(b)} \langle \bar{q}(Q^2)\rangle_n^{(b)} \exp[\frac{8}{3}\pi^2 \frac{\alpha(Q^2)}{4\pi}] \quad . \qquad (4.54)$$

In Eq.(4.54) only the π^2 terms related to the space-like, time-like mismatch have been kept. Expanding the last factor in Eq.(4.53) in power of $\alpha(Q^2)$ we reproduce the $8\pi^2/3$ term in Eq.(4.50). Similar methods have been discussed in refs.[126].

We think that this method of summing the π^2 terms related to the continuation in Q^2 is quite reasonable. It should be however kept in mind that not all π^2 terms are Summed by this method (e.g., the π^2 terms of Eq.4.51).

The exponential factor in Eq.(4.54) leads to a considerable change in the normalization of $\sigma_n^{q\bar{q}}(Q^2)$ as compared with the standard Drell-Yan formula, in which case this factor is equal unity. Choosing Λ=0.4 GeV and four active flavours the change of normalization is 2.2 and 1.6 for Q^2=10 GeV^2 and Q^2=100 GeV^2 respectively. This change of normalization is required by the data [212]. Do these data indicate the presence of higher order corrections?

4.6.3 Summing $(\log n)^2$ Terms. It has been suggested by various authors [8,141,145-147] that the most important higher order effects for large x(z) or large n can be taken into account already in the leading order calculations by using appropriately the kinematical bounds for the $k_\perp$ of the soft gluons. This does not mean of course that in the calculations discussed so far a wrong kinematics has been used. It should be however remembered that in the standard approach in which the expansion in $\alpha(Q^2)$ is made the quantities like $[\log Q^2(1-z)/\Lambda^2]^{-1}$ are replaced by

$$\frac{1}{\log Q^2/\Lambda^2(1-z)} = \frac{1}{\log Q^2/\Lambda^2}\left[1 - \frac{\log(1-z)}{\log Q^2/\Lambda^2} + O((\log Q^2/\Lambda^2)^{-2})\right] \tag{4.55}$$

$$\simeq \alpha(Q^2)\left[1 + \log(1-z)\alpha(Q^2) + O(\alpha^2(Q^2))\right] \quad . \tag{4.56}$$

The first term corresponds then to the leading order (in logarithms), the second term to the next-to-leading order and so on. Effectively then at each order the bound $k_\perp^2 \leq Q^2$ is used instead of $k_\perp^2 \leq (1-z)Q^2$ as required for instance in $e^+e^- \to h+X$. For z large enough so that $|\log(1-z)|\alpha(Q^2) \not\sim O(1)$ the expansion in Eq.(4.56) breaks down and resummation to all order has to be done. The example above indicates that maybe by rescaling the argument of the running coupling constant from Q^2 to $Q^2(1-z)$ one could automatically resum the series and take into account most important higher order corrections. It has been in fact suggested [146] that the following modification of the (leading order) evolution equations for fragmentation functions can accomplish it:

$$\frac{dD^{NS}(z,Q^2)}{d(\ln Q^2)} = \frac{\alpha(Q^2)}{2\pi}\int_z^1 \frac{dy}{y}[P(y)]_+ D(\frac{z}{y},Q^2) \tag{4.57}$$

$$\to \frac{1}{2\pi}\int_z^1 \frac{dy}{y}[P(y)\alpha(Q^2(1-y))]_+ D(\frac{z}{y},Q^2) \quad . \tag{4.58}$$

Here P(y) is the Altarelli-Parisi-DDT kernel and

$$[P(y)]_+ \equiv P(y) - \delta(1-y)\int_0^1 dx\, P(x) \quad . \tag{4.59}$$

A similar modification is suggested for quark distributions with (1-z) replaced by (1-x)/x.

The implications of these equations are as follows [146]

i) for finite (non-zero) n or x(z) away from 0 or 1 the standard evolution equations apply.

ii) for $1<<n<Q^2/Q_0^2$ or roughly $1-x>Q_0^2/Q^2$ the standard factor (see (4.19))

$$\left[\frac{\alpha(Q^2)}{\alpha(Q_0^2)}\right]^{d_n^{NS}} \underset{\text{large } n}{\approx} \exp\left[-\frac{16}{3\beta_0}\log n \log\frac{\alpha(Q_0^2)}{\alpha(Q^2)}\right] \equiv L_0^n \quad , \tag{4.60}$$

is replaced by

$$L_n^{NS}(Q^2,Q_0^2) = L_0^n \exp\left[-\frac{16}{3\beta_0}\left(-\log n + \log\frac{Q^2}{n\Lambda^2}\log\frac{\alpha(Q^2/n)}{\alpha(Q^2)}\right)\right] \quad . \tag{4.61}$$

Here Q_0^2 is $O(1\ GeV^2)$ but large enough so that $\alpha(Q_0^2)/2\pi \lesssim 1$. Furthermore to obtain (4.60) we have used the following large n behavior of d_n^{NS} (see Eq. 4.33)

$$d_n^{NS} = \frac{4}{3\beta_0}\left[1 - \frac{2}{n(n+1)} + 4\sum_{j=2}^{n}\frac{1}{j}\right] \to \frac{16}{3\beta_0}\log n \quad . \tag{4.62}$$

Taking $\alpha_s(Q^2)\log n \ll 1$ but $\alpha_s(Q^2)(\log n)^2 \gtrsim O(1)$ one obtains

$$L_n^{NS}(Q^2,Q_0^2) = L_0^n \exp\left[\frac{8}{3}\frac{\alpha(Q^2)}{4\pi}(\log n)^2\right] \quad , \tag{4.63}$$

i.e., exponentiation of the dominant part of the next to leading order correction as given by (4.23), (4.36) and (4.41).

iii) for $n > Q^2/Q_0^2$ or roughly $(1-x) < Q_0^2/Q^2$ one finds

$$L_n^{NS}(Q^2,Q_0^2) = F^2(Q^2,Q_0^2) = \exp\left[-\frac{16}{3\beta_0}\left(\log\frac{Q^2}{\Lambda^2}\log\frac{\alpha(Q_0^2)}{\alpha(Q^2)} - \log\frac{Q^2}{Q_0^2}\right)\right] \tag{4.64}$$

which has a form of the Sudakov formfactor [142,144,148] (see Section 7). In $e^+e^- \to h+X$ $F^2(Q^2,Q_0^2)$ is the probability that a photon of virtual mass Q^2 produces a single energetic $q\bar{q}$ pair plus an arbitrary number of soft gluons. The proprties i)-iii) apply to both the nonsinglet parton distributions and the nonsinglet fragmentation functions. But

iv) for very small n due to different kinematical bounds for $k_\perp^2$ the behavior of parton distributions and fragmentation functions is different. This is already seen in Fig. 19. Further details on this region can be found in [146,149].

Note that $L_n^{NS}(Q^2,Q_0^2)$ can be compactly written as follows [146]

$$L_n^{NS}(Q^2,Q_0^2) = \begin{cases} F^2(Q^2,Q_0^2)/F^2(\frac{Q^2}{n},Q_0^2) & n \lesssim \frac{Q^2}{Q_0^2} \\ F^2(Q^2,Q_0^2) & n > \frac{Q^2}{Q_0^2} \end{cases} . \tag{4.65}$$

Note also that Eq.(4.64) predicts a very strong damping (faster than any power of Q^2) at large x. Thus at large x there is still another reason why the leading twist contributions discussed here are probably less important than higher twist contributions.

This technique can also be used to sum the large $(\log n)^2$ corrections to massive muon production (see 4.50). In fact the appearance of $[\log n]^2$ terms in (4.50) can be shown to be due to the mismatch in the kinematical bounds on $k_\perp^2$ of gluons emitted in the massive muon production and the deep-inelastic scattering.

At present there is no proof that the equations like (4.58) take into account all dominant logarithmic corrections to all orders in perturbation theory. But the approach is very interesting. Further study in this direction is important.

4.7 Other Higher Order Calculations

There have been a few more higher order QCD calculations in the literature. We just list them now.

1. Contribution of $q+q \to q+q+\gamma^*$ ($O(\alpha^2)$) to the mass distribution in the massive muon production [150,151].
2. Contribution of $q+q \to q+q+\gamma^*$ to the $p_\perp$ distributions in the massive muon production [152].
3. Contribution of $q+q \to q+q+\gamma$ to the production of large $p_\perp$ real photons [153,154].
4. Next-to-leading order corrections to the one-hadron inclusive process $h+h \to h+$anything [155]. The Born diagrams are calculated in [156,157,158].
5. Next-to-leading order corrections to $h+h \to$ jet +anything [159].
6. Four jet calculations in e^+e^- annihilation [160,161].

The next-to-leading order corrections listed under 1, 2 and 3 are only large at kinematical boundaries. These large corrections can be presumably handled by the methods of Section 4.6. The origin of large QCD corrections to processes listed under 4,5 and 6 is however not understood at present.

Finally we should mention a very important finding of Doria, Frenkel and Taylor [162]. These authors made a study of the infrared behavior of the inclusive process $qq \to$ virtual photon+anything ($O(\alpha^2)$). Their study has been repeated by Di'Lieto, Gendron, Halliday and Sachrajda [163] who, although

finding some errors in the intermediate steps of the calculations of Ref.[162], confirmed the main result of Doria et al: for the process in question the Block-Nordsieck cancellation of infrared divergences (see Section 4.1) fails. The left infrared divergence is $O(m^2/Q^2)$ and will undoubtedly complicate the study of higher twist contributions to massive muon production. Generally a similar feature is expected for processes with two hadrons in the initial state [162-166]. The above results raise the following important question: does Bloch-Nordsieck mechanism work for leading twist contributions to the processes in question in order α^k with $k>2$?

4.8 Miscellaneous Remarks

In this section we have given a review of higher order QCD corrections to various semi-inclusive processes. Now a few remarks on the phenomenology of these processes are in order.

The Q^2 evolution of the fragmentation functions as measured in semi-inclusive deep-inelastic scattering has been studied in refs.[140,167,168]. It has been found that the data agree very well with the leading order QCD predictions. The question is then what happens beyond the leading order. We have not yet studied this question in detail but the following observation is maybe worth while mentioning. In spite of the fact that $[R_n^{NS}]_T > [R_n^{NS}]_S$ (see Fig. 19) the

next-to-leading order corrections to the ratio P_n^m of Eq.(2.29) are much smaller in the case of $e^+e^-\to hX$ than for deep-inelastic scattering (Table II). For instance $P_4^6=1.32$ and $P_4^8=1.56$.

The authors of refs.[140.167,168] have also found non-factorization in x and z in their data in a qualitative agreement with QCD predictions. More study in this direction is however needed. In particular in refs.[140,167,168] the next-to-leading order corrections to the parton distributions and fragmentation functions have not been taken into account. Furthermore it should be mentioned that non-factorization in question can also be caused by higher twist contributions (Section 5).

Of interest is also the large renormalization effect found in the massive muon production both in the theory and in the data [212]. More study of this effect is however needed before we can claim that the factor 2 (relative to the Drell-Yan prediction) found in the data is indeed a QCD effect.

5. Higher Twists

At low values of Q^2 one has to worry in addition to logarithmic scaling violtions about power-like scaling violations. In perturbative QCD they are represented by contributions of operators of higher twist. In the presence of higher twist contributions, Eq.(2.10) generalizes to

$$M^{NS}(n,Q^2) = \sum_{\substack{t=2 \\ \text{even}}} \frac{\tilde{A}_2^{(t)}}{[Q^2]^{t-2}} [\alpha(Q^2)]^{d_2^{(t)}} [1 + R_n^{(t)} \frac{\alpha(Q^2)}{4\pi} + \ldots] \quad . \tag{5.1}$$

where the sum runs over various twist ($\underline{t}$) contributions: leading twist (t=2), twist four (t=4) and so on. $\tilde{A}_n^{(t)}$ are incalculable hadronic matrix elements of spin n, twist t operators. $d_n^{(t)}$ and $R_n^{(t)}$ are calculable numbers; eq., $d_n^{(2)}=d_n^{NS}$ and $R_n^{(2)}=R_n^{NS}$.

Let us summarize what is known at present about the higher twist contributions.

a) There are many operators of a given twist>2 contributing to Eq.(5.1) so this equation is in reality more complicated than we have shown. Consequently there are many unknown non-perturbative parameters $A_n^{(t)}$ (t>2) which have to be extracted from the data. This makes the phenomenology of higher twist contributions very complicated. The situation might be considerably simplified in certain regions of phase-space (e.g., x→1) and for particular cross-sections in

which case one can identify and calculate the dominant higher-twist contributions [8,169,170].

b) The anomalous dimensions of some of the twist four (t=4) operators have been calculated in refs.[171] and [172]. The two novel features as compared with $d_n^{(2)}$ are as follows. $d_n^{(4)}$ can be negative as opposed to $d_n^{(2)} \geq 0$. Furthermore whereas $d_n^{(2)} \sim \log n$ for large n, the $d_n^{(4)}$ may increase faster with n. These two features indicate that the structure of logarithmic corrections to higher twist contributions might be much more complicated than in the case of the leading twist. It would be interesting to study numerically these effects.

c) Since the parameters $A_n^{(t)}$ are incalculable at present (see however below) one can study phenomenologically the effects of higher twist contributions in deep inelastic scattering by using "QCD motivated" parametrizations of the terms t>2 in Eq.(5.1).

An analysis of this type has been done one year ago by Abbott and Barnett [173], who found that the deep-inelastic data can be fit by higher twist contributions alone. Their combined analysis of twist 2 and higher twist contributions indicated that the value of the parameter Λ is strongly dependent on the size of higher twist contributions. If the latter increase the Λ decreases. Similar analysis has been done by Perkins [174].

Recent analyses of Duke and Roberts [175] and Pennington and Ross [176] who combine all the existing data show however that the best fits to the data can be obtained if the higher twist contributions are small (see however [177]).

In judging these results we should keep in mind that these analyses do not prove that the real QCD higher twist contributions are small. To prove it one had to calculate the non-perturbative parameters $A_n^{(t)}$ of Eq.(5.1) and show that $A_n^{(t)}$'s with $t>2$ are sufficiently small. Furthermore even if higher twist contributions may appear to be of little importance in the analysis of deep-inelastic structure functions for $Q^2>5$ GeV^2 and $x>0.8$, they may be and they probably are important for $x\to 1$.

d) We have seen that our understanding of the importance of higher twist contributions could be substantially improved if we could estimate the parameters $A_n^{(t)}$. At present this can only be done in the context of specific models. In particular an estimate of the twist two matrix elements ($A_n^{(2)}$) in the bag model has been done recently by Jaffe and Ross [64], who find that the parameters $A_n^{(2)}$ are in a very good agreement with the low Q^2 ($\sim$1 GeV^2) deep-inelastic data. We may then conclude that the full (twist two plus higher twist contributions) result for deep-inelastic structure functions in the bag model can only agree with the data if the higher twist contributions are small. As a consistency check at least the calculation of the matrix elements $A_n^{(4)}$ should be done. Such a calculation although feasible is

however very difficult. One may of course ask how much the bag model has to do with QCD? In spite of this the analysis of ref.[64] is very interesting and undoubtedly one should pursue in this direction with the hope of gaining a better understanding of higher twist contributions.

e) The question of power corrections to various semi-inclusive processes and also to processes of the type (1.2) has also been addressed in the literature [178,180]. In particular it has been conjectured [180] that the general structure of higher twist contributions will be analogous to that of leading twist contributions with parton distributions and parton fragmentation functions (referred to as single longitudinal functions) replaced by multi-longitudinal functions, which involve several partons at the same time. Much work however has still to be done before this approach can be put on the same footing with the leading twist perturbative QCD of Sections 2-4. In particular a general proof of factorization of mass singularities is missing for power corrections. Undoubtedly a theoretical study of power corrections will be complicated by the findings of refs.[162-166] that the Bloch and Nordsiek theorem [95] fails for non-abelian theories at the m^2/Q^2 level.

f) We should also mention interesting calculations of higher twist contributions to pion structure functions [169] and to quark fragmentation functions into π [170]. The former lead to sizable effects in the angular distribution of heavy muon pairs produced in hadron-hadron collisions. The

latter induce z and $y=(E_\nu-E_\mu)/E_\nu$ correlation in semi-inclusive cross-sections such as $\nu N \to \mu^- \pi^+ X$ and $\bar{\nu} N \to \mu^+ \pi^- X$. Both effects have been seen in the data ([8],[181]). More study is however neded before one can claim that the effects seen in the data are due to higher twist contributions and not to higher order QCD corrections to leading twist predictions.

6. Exclusive Processes

6.1. Preliminary Remarks

In the past year there has been a lot of progress in the understanding of QCD effects in exclusive processes. These include elastic form factors, transition form factors, elastic scattering at fixed angle and deep inelastic structure functions for $x \to 1$. Since these topics have been covered in detail at this Symposium by Stan Brodsky [182] and Tony Duncan [183], we shall here only present the basic structure of QCD formulae for exclusive processes and list the most important results.

Let us begin by recalling the well known counting rules [184,185]. They are:

a) For spin-averaged form factors at $|t| >> M^2$

$$F_h(t) \sim \frac{1}{t^{n-1}} , \tag{6.1}$$

where n is the number of constituent fields in the hadron h.

b) For fixed angle scattering at $t >> M^2$, t/s fixed

$$\frac{\sigma}{dt} (AB \to CD) \sim \frac{1}{t^{\tilde{n}-2}} f(\frac{t}{s}) , \tag{6.2}$$

where $\tilde{n}$ is the total number of consitituent fields in hadrons A,B,C and D.

c) For deep inelastic structure functions at $Q^2 >> M^2$ and $(1-x)Q^2/x$ fixed

$$F_2^h(x,Q^2) \sim (1-x)^{2n_s-1} , \tag{6.3}$$

where n_s is the number of spectator fields in the hadron h.

For instance n=2, $\tilde{n}$=10 and n_s=1 for F_π, $\pi p \to \pi p$ and F_2^π respectively. The dominant diagrams responsible for these counting rules are shown in Fig. 23.

At this stage one should also mention

d) Landshoff diagrams [186], which are shown in Fig. 24 and which lead for instance to

$$\left(\frac{d\sigma}{dt}\right)_{\pi\pi} \sim \frac{1}{t^5} , \tag{6.4}$$

as opposed to $1/t^6$ predicted by Eq. (6.2). Thus for large t the diagrams of Fig. 24 should dominate (in the absence of QCD effects) over the dimensional counting contributions.

In QCD three things happen:

1) the counting rules a) and b) although verified are modified by calculable logarithmic corrections,
2) the Landshoff diagrams turn out to be suppressed by Sudokov form factors and are less important at large t than the dimensional counting contributions, and
3) the counting rule c), although verified (except for

logarithmic corrections) for the proton, fails for the pion.

There are many authors [8, 186-198] who contributed to the understanding of QCD effects in exclusive processes, but the most extensive study has been done by Brodsky and Lepage [197]. We shall follow here their approach. A more formal discussion of exclusive processes can be found in refs. [191, 193, 194].

6.2. Basic Structure

We have seen in Sections 2 and 4 that the basic elements of any QCD formula for inclusive and semi-inclusive processes were

i) universal Q^2 dependent parton distributions and parton fragmentation functions for which only the Q^2 evolution was calculable,

and

ii) process dependent elementary parton cross-sections (short distance functions), which were calculable in perturbation theory.

Similarly the basic elements of any QCD formula for exclusive processes are

i') universal Q^2 dependent "parton distribution amplitudes" $\phi(x_i,Q^2)$ for which only the Q^2 evolution is calculable,

and

ii') process dependent hard scattering amplitudes $T_H(x_i,\ldots)$

which are calculable in perturbation theory.

In analogy with Eqs. (4.2) and (4.3) we have

$$F_{\pi\gamma}(Q^2) = \int_0^1 [dx]\ T_H(x_i,Q^2)\phi_\pi(x_i,Q^2)\ , \tag{6.5}$$

for π-γ transition form factor,

$$F_h(Q^2) = \int_0^1 [dx][dy]\phi_h^*(y_i,Q^2)T\ (x_i,y_i,Q^2)\phi_h(x_i,Q^2), \tag{6.6}$$

for the electromagnetic form factor of a hadron h, and

$$M(AB\to CD) = \int_0^1 \prod_{i=a,b,c,d} [dx_i]\phi_C^*(x_c,p_\perp^2)\phi_D^*(x_d,p_\perp^2)$$
$$\cdot\ T_H(x_i,s,\theta_{c.m.})\phi_A(x_a,p_\perp^2)\phi_B(x_b,p_\perp^2) \tag{6.7}$$

for the fixed angle scattering amplitude as $s\to\infty$ ($p_\perp^2 = \frac{tu}{s}$). $[dx]\equiv dx_1dx_2\delta(1-x_1-x_2)$ in Eq. (6.5), and stands for analogous expressions in Eqs. (6.6-6.7). Equations (6.5)-(6.7) are shown schematically in Fig. 25, where (in analogy with Fig. 17) the circles stand for $\phi(x_i,Q^2)$, the squares denote the amplitudes T_H and the connecting internal lines stand for quarks or antiquarks. Only the dominant components of the hadronic wave functions ($q\bar{q}$ for mesons and qqq for baryons) are shown in Fig. 25. The components with more fermions

(eg. $q\bar{q}$ $q\bar{q}$ for mesons) are suppressed by at least one power of Q^2. In general, components containing gluons (e.g. $q\bar{q}$ + several gluons) are not suppressed, but in the light-cone gauge used in ref. [197] these components are also down by powers of Q^2. The generalization to other gauges can be found in the Appendix C of ref. [197].

6.2.1. Parton Distribution Amplitudes

The quark distribution amplitude $\phi_h(x_i,Q^2)$ is the amplitude for finding constituents with the longitudinal momentum fractions x_i in the hadron h which are collinear up to the scale Q^2. $\phi_h(x_i, Q^2)$ is related to the hadronic wave function $\psi_h(x_i,k_\perp)$ by the following equation

$$\phi_h(x_i,Q^2) \sim \int^{Q^2} dk_\perp^2 \, \psi_h(x_i,k_\perp) \ . \tag{6.8}$$

The Q^2 dependence of $\phi_h(x_i,Q^2)$ is specified by an evolution equation [189,197] which in the leading order is given as follows

$$Q^2 \frac{\partial}{\partial Q^2} \phi_h(x_i,Q^2) = \frac{\alpha(Q^2)}{4\pi} \int_0^1 [dy] V_h(x_i,y_i) \phi_h(y_i,Q^2) \ . \tag{6.9}$$

The function $V_h(x_i,y_i)$ can be computed from a single gluon exchange kernel. It is the analog of the Altarelli-Parisi

function P_{qq} [50] which enters the evolution equations for the non-singlet quark distributions. The explicit expressions for $V_\pi(x_i,y_i)$ and $V_B(x_i,y_i)$ (B=baryon) can be found in ref. [197]. From (6.9) one obtains for instance

$$\phi_\pi(x_i,Q^2) = x_1x_2 \sum_{n=0,2,4,\ldots}^{\infty} a_n\, C_n^{3/2}(x_1-x_2)\left[\ln\frac{Q^2}{\Lambda^2}\right]^{-d_{n+1}^{NS}} \tag{6.10}$$

where d_{NS}^n are the anomalous dimensions of Eq. (2.5) and $C_n^{3/2}$ are Gegenbauer polynomials. The coefficients a_n can be determined from $\phi_\pi(x_i,Q_0^2)$, which has to be taken from data at some arbitrary (not too small) value of $Q^2=Q_0^2$,:

$$a_n = \left[\ln\frac{Q_0^2}{\Lambda^2}\right]^{d_{n+1}^{NS}} \frac{2(2n+3)}{(2+n)(1+n)} \int_{-1}^{1} d(x_1-x_2)C_n^{3/2}(x_1-x_2)\phi_\pi(x_i,Q_0^2)\ , \tag{6.11}$$

since $d_1^{NS}=0$ and $d_n^{NS}<0$ for $n>1$ one obtains for $Q^2\to\infty$

$$\phi_\pi(x_i,Q^2) \to a_0x_1x_2 = \sqrt{3}\, f_\pi x_1x_2, \tag{6.12}$$

where f_π=93 MeV is measured in the decay $\pi\to\mu\nu$. Equations (6.10) and (6.11) apply also to other mesons. Analogs of these equations for $\phi_B(x_i,Q^2)$ can be found in [197].

6.2.2. Hard Scattering Amplitudes

T_H in the case of the pion form factor is the amplitude for scattering of a $q\bar{q}$ system with the photon to produce q and $\bar{q}$ in the final state whose momenta are roughly collinear. In lowest order one obtains

$$T_H(x_i,y_i,Q^2) = \frac{16\pi\ C_F\alpha(Q^2)}{Q^2}\ \frac{1}{x_2y_2}\ , \tag{6.13}$$

where $C_F=4/3$.

The corresponding amplitudes relevant for $F_{\pi\gamma}$ and F_B are given in [197].

6.3 Basic Results

Expressions (6.10) and (6.13) and analogous expressions relevant for $F_{\pi\gamma}$, F_B and M(AB→CD) can now be inserted into the general formulae (6.5)-(6.7). One obtains [197] (leading order)

$$F_{\pi\gamma}(Q^2) = \frac{2}{\sqrt{3}}\ \frac{1}{Q^2}\ \sum_{n=0,2,4} a_n\left[\ln\frac{Q^2}{\Lambda^2}\right]^{-d^{NS}_{n+1}}\ , \tag{6.14}$$

$$F_\pi(Q^2) = 4\pi C_F\ \frac{\alpha(Q^2)}{Q^2}\ \left|\ \sum_{n=0,2,4} a_n\left[\ln\frac{Q^2}{\Lambda^2}\right]^{-d^{NS}_{n+1}}\right|^2\ , \tag{6.15}$$

$$G_M(Q^2) = \frac{32\pi^2}{9}\ \left(\frac{\alpha(Q^2)}{Q^2}\right)^2\ \sum_{n,m} b_{nm}\left[\ln\frac{Q^2}{\Lambda^2}\right]^{-d^{NS}_{n+1}-d^{NS}_{m+1}}\ , \tag{6.16}$$

and

$$\frac{d\sigma}{dt}(AB\to CD) \underset{\substack{\text{large } s \\ \text{large } p_\perp^2}}{\to} \left[\frac{\alpha(t)}{t}\right]^{\tilde{n}-2} \left(\ln \frac{p_\perp^2}{\Lambda^2}\right)^{-2\sum_i \gamma_i} f(\theta_{c.m.}), \qquad (6.17)$$

where γ_i depend on the spin of the hadron. For pions $\gamma_i=0$, while for protons $\gamma_i=-2/3\beta_0$. $G_M(Q^2)$ stands for proton's magnetic form factor. Equation (6.15) has also been obtained in ref. [192]. The coefficients b_{nm} can be determined from $\phi_p(x_i,Q_0^2)$ which has to be taken from the data. In order to find $f(\theta_{c.m.})$ the $\theta_{c.m.}$ dependence of T_H which enters Eq. (6.7) must be known. Unfortunately such a calculation is very difficult and even in the leading order involves millions of diagrams. The large number of diagrams contributing to hard scattering sub-processes discussed above, may however explain why these sub-processes dominate in wide angle scattering over the Landshoff contributions [186]. Furthermore as has been shown in refs. [197] and [198] the latter contributions are in QCD suppressed by Sudakov form factors [199] which fall faster than any power of t as $-t\to\infty$. We shall discuss Sudakow form factors briefly in Section 7.

Comparing Eqs. (6.14)-(6.17) with Eqs. (6.1) and (6.2) and taking into account the suppression of Landshoff diagrams we observe that the counting rules a) and b) are verified except for logarithmic corrections. How important are these corrections? This has been discussed in detail by Stan Brodsky, so let us only list a few important points

i) Note that the asymptotic behaviour of the pion form factor is fixed (see Eq. (6.12)):

$$F_\pi(Q^2) \to 16\pi f_\pi^2 \frac{\alpha(Q^2)}{Q^2} = \frac{\alpha(Q^2)}{Q^2} [0.43 \text{ GeV}^2] . \qquad (6.18)$$

Evaluating equation (6.18) at $Q^2=4$ GeV^2 and using $\Lambda_{LO}=0.5$ GeV one obtains $Q^2F_\pi(Q^2) \gtrsim 0.2$ as compared to the experimental value 0.40 ± 0.08 [200]. Thus the terms with $n \neq 0$ must be important. Choosing $\phi(x_i,Q_0^2) \sim [x_1x_2]^{1/4}$ at $Q_0^2=2$ GeV^2 and $\Lambda_{LO}=0.40 \pm 0.10$ one obtains from (6.11) and (6.15) $Q^2F_\pi(Q^2)$ which is consistent with the available data at $Q^2 \leq 4$ GeV^2. (See Fig. 12 of ref. [197].) Present data are however not good enough to test the logarithmic QCD corrections to the pion form factor.

ii) Similar analysis shows that a value of $\Lambda<0.2$ GeV, preferrably $\Lambda<0.1$ GeV, is required to fit the experimental data [201] for $G_M(Q^2)$. In fact the data do not show almost any Q^2 dependence for $Q^4 G_M(Q^2)$ for $Q^2>5$ GeV^2.

iii) For elastic scattering due to the high power of $\alpha(t)$ in Eq. (6.17), the effective power of $1/t$ is modified relatively to the counting rules. This is illustrated in Table VII. Since the counting rules seem to agree well with experimental data [202] again a very small value of $\Lambda(<0.1)$ is required. This value is

substantially smaller than the one extracted from deep-inealstic scattering in the absence of higher twist contributions. Of course in order to make a meaningful comparison of scale parameter Λ extracted from deep-inelastic scattering with that obtained from wide angle scattering, the next to leading order corrections to the latter have to be calculated. This involves calculations of higher order corrections to the kernel $V_h(x_i,y_i)$ which enters the evolution equation (6.9) and similar calculations for the hard scattering amplitude T_H in (6.7). The latter calculations are particularly difficult.

6.4. Miscellaneous Remarks

Discussions of deep-inelastic structure functions for $x\to 1$ and $(1-x)/x\ Q^2$ fixed can be found in ref. [182], [183], [190], [192] and in particular in Section 8 of ref. [8]. Some aspects of this topic have also been discussed in Section 4.6 of the present paper.

It should also be remarked that the life might not be as easy as presented here. For possible complications, in particular in fixed angle scattering, we refer the reader to refs. [183], [193] and [194].

7. $p_\perp$ Effects

7.1 Preliminaries

Among the most spectacular QCD effects are $p_\perp$ effects which are caused by gluon bremsstrahlung. These have been most extensively studied in the massive muon production and in e^+e^- annihilation. We shall here concentrate on the massive muon production.

In the standard Drell-Yan model and in the absence of the primordial $k_\perp$ of annihilating quarks and antiquarks the transverse momentum $p_\perp$ of the muon pair is zero. In QCD $p_\perp$ is no longer zero and its perturbative component receives the dominant $O(\alpha)$ contribution from the diagrams of Figs. 18b,c and 26. The $p_\perp$ distributions resulting from these diagrams have been calculated by various authors ([101], [204-211]). The result is compared with the data [212] in Fig. 27. It is clear that the diagrams of Figs. 18 and 26 cannot reproduce the data. In particular the shape at small and intermediate $p_\perp$ is wrong. Furthermore at low $p_\perp$ the predicted distribution behaves as $1/p_\perp^2$ contrary to the data which is rather flat. For large $p_\perp^2 \sim O(Q^2)$ the situation is much better but the theoretical predication lies somewhat lower than the measured distribution.

A little thinking convinces us however that there is as yet no need to worry or to panic, and this for four reasons.

First there is something positive in the Fig. 27. The data show large $p_\perp$ effects in accordance with theoretical expectations. Furthermore the predicted increase of $\langle p_\perp^2 \rangle$ with s and Q^2 is confirmed by the data [212].

Second the theoretical predictions shown in Fig. 27 are based on the expressions like

$$\frac{d\sigma}{dQ^2 dp_\perp^2} \sim \frac{4\pi\alpha_{EM}^2}{9sQ^2} \int dx_1 dx_2 \; q(x_1,Q^2)\bar{q}(x_2,Q^2)\sigma(x_1,x_2,\tau,Q^2/p_\perp^2) \tag{7.1}$$

in accordance with the general procedure of Section 4.2. In the case of $p_\perp$ distributions this procedure only applies [113] for $p_\perp^2 \approx O(Q^2)$. If $p_\perp^2$ is $O(Q^2)$ at order α_s^n there is only an n-fold logarithmic divergence due to mass (collinear) singularities, while the infrared (soft) divergences cancel between real and virtual gluon corrections. As discussed in Section 4 the mass singularities can be factored out and the left over large logarithms $\alpha_s^n \log^n Q^2$ can be resummed to give Q^2 dependent parton distributions. Note that if only the leading logarithms in each order of perturbation theory are kept then as long as $p_\perp^2$ is $O(Q^2)$ it is irrelevant whether $p_\perp^2$ or Q^2 is the variable which the quark distributions depend on. Any difference between choosing $p_\perp^2$ or Q^2 can only be consistently treated once the next-to-leading logarithms are taken into account. For $p_\perp^2 << Q^2$ the situation is more complicated. Now at each order in perturbation theory the dominant corrections to the standard Drell-Yan process are of

the form $\alpha_s^n \ln^{2n}(Q^2/p_\perp^2)$ arising from the emission of n gluon which are both soft and collinear. If $Q^2 >> p_\perp^2$ the perturbation theory breaks down and these large logarithms have to be summed to all order of perturbation theory. Futhermore it is now relevant to find out whether it is Q^2 or $p_\perp^2$ which enters the evolution equations for parton distributions. We shall deal with these questions in Section 7.2. In any case we should not be surprised that the formula like (7.1) disagrees with data for $p_\perp^2 << Q^2$.

Third at low $p_\perp$ one may expect non-perturbative effects related to the intrinsic (primordial) $\langle k_\perp \rangle$ to be of importance. The usual procedure [204] is to convolute the perturbative result of Fig. 27 with the primordial distribution chosen to have the form

$$f(k_\perp^2) \sim \exp\left[-\frac{k_\perp^2}{2\langle k_\perp^2 \rangle}\right] \tag{7.2}$$

Choosing $\langle k_\perp \rangle$ 600 MeV one obtains a good agreement with the data. This procedure is however very ad hoc and the reached agreement with the data cannot be regarded as a success of the theory. Nevertheless the primordial $k_\perp$ effects should be somehow taken into account. How really they are important can only be answered once the perturbative part of the $p_\perp$ distributions at relatively low $p_\perp$(O(1 GeV)) is correctly taken into account. We shall come to this in Section 7.2.

Fourth one may ask whether the next-to-leading order QCD corrections which are here $O(\alpha_s^2)$ could modify substantially the leading order result of Fig. 27. In particular the subprocess $q+q\to q+q+\gamma^*$ could be of importance if the two initial quarks are valence quarks. Note that this process is expected to be more important for $p_\perp$ distributions than for mass distributions since the perturbative expansion for the latter begins in $O(\alpha^0)$ whereas the former begins in order α. Indeed it has been found in ref.[154] that the inclusion of the subprocess $q+q\to q+q+\gamma^*$ brings the QCD prediction for the $p_\perp$ distributions in massive muon production closer to the data especially at large $p_\perp$. Of course in order to complete the study of next-to-leading order corrections to $p_\perp$ distributions, other contributions of $O(\alpha_s^2)$ have to be evaluated.

7.2 Intermediate and Small $p_\perp$

The region $\Lambda^2 << p_\perp^2 << Q^2$ has been first studied by Dokshitzer et al. [213]. As we have remarked above, in this region large loarithms $\alpha^n \log^{2n}(Q^2/p_\perp^2)$ appear and the summation to all order in perturbation theory has to be performed. This has been done in ref.[213] with the following result (valid in the double leading logarithmic approximation, DLL)

$$\Sigma(p_\perp^2,Q^2) \equiv \int_0^{p_\perp^2} \frac{d\sigma}{dk_\perp^2 dQ^2}\, dk_\perp^2 \quad ,$$

$$= \sum_i e_i^2\, q(x_1,p_\perp^2)\bar{q}(x_2,p_\perp^2)S^2(p_\perp^2,Q^2) \quad . \qquad (7.3)$$

Here e_i are the quark charges, $q(x_1,p_\perp^2)$ and $\bar{q}(x_2,p_\perp^2)$ are parton distributions evaluated at $p_\perp^2$(not Q^2) and $S^2(p_\perp^2,Q^2)$ is the square of a formfactor (denoted in [213] by T^2) which the authors of ref.[213] found to be different from the Sudakov formfactor [199] (see 4.64). Subsequent analyses [214-221] have confirmed the general structure of Eq.(7.3) except that $S^2(p_\perp^2,Q^2)$ turned out to be indeed the square of the Sudakov form factor.

In the case of a fixed strong interaction coupling constant α one obtains (in DLL)

$$S^2(p_\perp^2,Q^2) = \exp[-\frac{2\alpha}{3\pi}\log^2(Q^2/p_\perp^2)] \quad , \qquad (7.4)$$

whereas when α is running

$$S^2(p_\perp^2,Q^2) = \exp[-\frac{16}{25}\log(Q^2/\Lambda^2)\log[\frac{\log Q^2/\Lambda^2}{\log p_\perp^2/\Lambda^2}] + \frac{16}{25}\log(Q^2/p_\perp^2)] \qquad (7.5)$$

Note that (7.5) can be obtained from (4.64) by putting there $\beta_0=25/3$, $Q_0^2=p_\perp^2$ and using the leading order formula for α.

It has been pointed out by Parisi and Petronzio [214] that the physics of $p_\perp^2 << Q^2$ can be easier studied in the impact parameter space rather than in the momentum space. In particular the exponentiation of soft gluon emissons which lead to large logarithms can be done directly in the b rather than $k_\perp$ space. Furthermore it is claimed in refs.[217] and [218] that such exponentiation in the b space can be proven to occur to all orders in perturbative theory and in all logarithms (leading next to leading and so on).

Defining $\tilde{\sigma}(b,Q^2)$ by

$$\frac{d\sigma}{dp_\perp dQ^2} = \frac{1}{4\pi} \int d^2b \, \exp[-i \vec{b}\cdot\vec{p}_\perp] \tilde{\sigma}(b,Q^2) \quad , \tag{7.6}$$

one obtains [214,218,220]

$$\tilde{\sigma}(b,Q^2) = \sum_i e_i^2 q(x_1,\frac{1}{b^2}) \bar{q}(x_2,\frac{1}{b^2}) \tilde{S}^2(b^2,Q^2) + O(\bar{g}^2(\frac{1}{b^2})) \quad , \tag{7.7}$$

where (in the leading order approximation)

$$\tilde{S}^2(b^2,Q^2) = S^2(p_\perp^2,Q^2)\Big|_{p_\perp^2=1/b^2} \tag{7.8}$$

with $S^2(p_\perp^2,Q^2)$ given by Eqs.(7.4) and (7.5).

Details of the calculations which lead to the formulae above can be found in refs.[214]-[221]. Here we shall only list some of the implications of these results and discuss

the physics behind it.

1. The formulae above are obtained by summing the diagrams of the type shown in Fig.28 with all emitted gluons being both soft and collinear to the incoming q and $\bar{q}$.

2. The occurrence of $\alpha^2 \log^{2n}(Q^2/p_\perp^2)$ terms is a consequence of the incomplete cancellation between soft virtual and real gluon emissions. Restricting $p_\perp^2$ of the muon pair to the values much smaller than Q^2 puts also a restriction on $k_\perp$ of the emitted gluons in the real diagrams. There is no such restriction for virtual diagrams. Hence incomplete cancellation.

3. The formfactor S^2 plays the role of an effective quark formfactor and it gives the probability for massive (Q^2) muon pair production in $q\bar{q}$ annihilation without emission of gluons having $k_\perp$ greater than $p_\perp$. When $p_\perp^2 << Q^2$ this probability is very small.

4. In the impact parameter space one can distinguish three regions ([214],[218])

i) $0 \leq b^2 \leq 1/Q^2$ in which the standard perturbative calculations (see 7.1) are justified,

ii) $1/Q^2 \leq b^2 \leq 1/\Lambda^2$ in which the formulae of this section apply,

and

iii) $b^2 \geq 1/\Lambda^2$ in which non-perturbative effects become important.

It has been pointed out [214] that the contribution from the

last region to the integral in Eq.(7.6) tends to zero faster than any power of Q^2 (see also point 3 above). Consequently at large Q^2 the $p_\perp$ distribution is dominated by the two first regions, and is calculable even for small values of $p_\perp^2$. Correspondingly the sensitivity to the intrinsic $k_\perp$ is lost at large Q^2.

5. Note that $S^2(p_\perp^2,Q^2)$ as given by Eqs.(7.4) and (7.5) has the shape in $p_\perp$ opposite to the one obtained on the basis of the lowest order diagrams of Figs.18 and 26 (see Fig.27). Therefore the inclusion of soft gluon emissions into the phenomenological analysis helps [213,214] to explain the shape of the $p_\perp$ distributions seen in the data.

7.3 Outlook

The next step is to study the effects of non-leading logarithms which arise for instance from diagrams of Fig. 28 with some of the emitted gluons being non-soft or noncollinear to the incoming q and $\bar{q}$. The study of these effects is just beginning [142,144,216,218]. In particular in ref.[218] a systematic procedure for the study of these effects has been suggested. It is also important to connect smoothly the regions i)-iii) discussed above. Progress in this direction has been made in refs.[218] and [219].

One should also remark that the effects of the quark formfactor discussed here can also be studied in other processes [213,216,222]. In particular in ref.[216] it has

been suggested that the quark formfactor can be better "seen" in e^+e^- annihilation than in the massive muon production. A recent phenomenological study of quark formfactor effects in e^+e^- annihilation is given in [223].

8. Jetology and Photonology

Our last (seventh on our list) topic deals with jets and photons. Each of these two topics could constitute a separate review of the length of the present one. Because of lack of time we shall here only make a few remarks.

During the last few years there have been literally hundreds of papers which deal with jet physics. These are reviewed in refs.[5-12,224,225]. Let us just list some of the latest theoretical achievements in this field.

1) Calculations of higher order corrections to Sterman-Weinberg formula [115,226]. In particular Duncan, Gupta and Mueller[115] have developed a renormalization group approach which allows a systematic study of higher order corrections to single jet Sterman-Weinberg cross-sections.

2) Summation of leading logs in thrust distributions ($T\approx 1$) [227].

3) Four jet calculations [160,225,228] and general investigation of higher order effects. These are important for the determination of the effective coupling constant and for the tests of the non-abelian nature of QCD [229], [225].

4) Generalization of the jet calculus to include exact kinematical constraints [230,231] and a detailed study [231] of preconfinement [232].

5) Extension of the jet calculus [233] beyond the leading order [136], [234].

6) A study of the multi-jet structure in QCD [235], and

7) Further study of hadronization effects [236],[10].

Other theoretical achievements and the comparison with experimental data can be found in the quoted reviews.

During the last few years there has been a lot of interest in the study of processes involving real and almost real photons. Let us just mention some of the attractive features of photon physics.

1) The photon-photon collisions (see Section 3) become an increasingly important source of hadrons in e^+e^- collisions as the center of mass energy is raised. In fact, in the LEP region these processes will be more important than the standard annihilation process.

2) In particular the proceduction of high $p_\perp$ jets in $e^+e^-\to e^+e^-X$ becomes important at LEP energies [83,84,237].

3) The structure of QCD formulae for semi-inclusive processes involving photons are similar to the one presented in Section 4 except that the parton distributions in hadrons and fragmentation functions into hadrons are replaced by the corresponding distributions for photons. Since the latter (see Section 3) are at large Q^2 exactly computable, the number of free parameters in processes involving photons is substantially smaller than in the corresponding processes involving hadrons.

4) Because the parton distributions in a photon are much harder than the corresponding distributions in hadrons, one finds that the photon beams are much more efficient than

hadron beams at producing high $p_\perp$ events [238].

5) The production of direct photons in hadron hadron collisions should also become incresingly important [239].

Photon physics has been reviewed in refs. [8,83,84,240].

9. Summary

In this review we have discussed QCD predictions for inclusive and semi-inclusive processes with particular emphasis put on higher order corrections. Also a discussion of exclusive processes and of $p_\perp$ effects has been given.

While discussing higher order effects we have stressed the following new features not encountered in the leading order:

i) gauge and renormalization-prescription dependences of separate elements of the physical expressions;

ii) freedom in the definition of $\alpha(Q^2)$;

iii) freedom in the definition of parton distributions and parton fragmentation functions beyond the leading order approximation.

These features have to be kept in mind when carrying out calculations to make sure that various parts of the higher order calculations are compatible with each other. Only then can a physical result be obtained which is independent of gauge, renormalization scheme, particular definition of $\bar{g}^2(Q^2)$, and particular definitions of the parton distributions and fragmentation functions.

We have seen that the higher order corrections are sometimes large (in particular at kinematical boundaries) and a resummation of them has to be made.

In spite of the fact that a lot of progress has been done during the last seven years in the understanding of QCD effects in various processes, still many outstanding questions have to be answered. A partial list of topics which deserve futher study is as follows:

1) Power corrections (higher twists) in inclusive and semi-inclusive processes.

2) The study of power corrections in hard scattering processes with two incoming hadrons will be complicated by the findings of refs. [162-166] that the Block-Nordsieck cancellation of infrared divergences (see Section 4.1) does not occur in these processes at m^2/Q^2 level. Further investigation of the results of refs.[162-166] is of great importance.

3) Calculations of higher order corrections to exclusive processes.

4) Further study of Sudakov-like effects (Section 7) in various processes.

5) More phenomenology of higher order corrections in particular for processes for which these corrections are large and a resummation of these corrections is needed.

6) Further exploration of photon physics.

7) Further study of spin effects [241-243], [62].

8) Better understanding of non-perturbative effects, and many others.

Seven exciting years have passed. We are looking forward to the seven years to come during which many of the problems listed above will be solved and many new questions will be asked.

Acknowledgments

In preparing these notes I have benefitted from discussions with Bill Bardeen, John Collins, Dennis Duke, Charles Nelson, and Norisuke Sakai. I would also like to thank Paul Hoyer and Jens Lyng Petersen for inviting me to this exciting, in many respects, symposium. Finally, it is a pleasure to thank Elaine Moore and Pat Oleck for typing this rather lengthy manuscript.

References

1. H.D. Politzer, Phys. Rev. Lett. 30, 1346 (1973); D.J. Gross and F. Wilczek, Phys. Rev. Lett. 30, 1323 (1973); G. 't Hooft, unpublished.
2. A. Peterman, Phys. Rep. 53C, 157 (1979).
3. A.J. Buras, Rev. Modern Phys. 52, 199 (1980).
4. Y.L. Dokshitzer, D.I. Dyakonov and S.I. Troyan, Phys. Rep. 58C, 269 (1980);
5. J. Ellis and C.T. Sachrajda, TH.2782-CERN. J. Ellis, Proceedings of the 1979 International Symposium on Lepton and Photon Interactions at High Energies, Fermilab, 1979 ed. T.B.W. Kirk and H.D.I. Abarbanel.
6. S.D. Ellis, in "Quantum Flavordynamics, Quantum Chromodynamics and Unified Theories," ed. K.T. Mahanthappa and J. Randa, Plenum Press, p. 139 (1980).
7. R.D. Field, in "Quantum Flavordynamics, Quantum Chromodynamics and Unified Theories," ed. K.T. Mahanthappa and J. Randa, Plenum Press, P. 221 (1980).
8. S.J. Brodsky and G.P. Lepage, SLAC-Pub-2447 (1979).
9. E. Reya, DESY 79/88 (1979).
10. P. Hoyer, Nordita-79/33 (1979).

11. K. Konishi, CERN preprints, TH.2853,2897-CERN (1980).

12. C.H. Llewellyn-Smith, Proceedings of the 1980 International Conference on High Energy Physics, Madison, (1980).

13. W. Caswell, Phys. Rev. Lett. 33, 244 (1974).

14. D.R.T. Jones, Nucl. Phys. B75, 531 (1974).

15. H. Georgi, and H.D. Politzer, Phys. Rev. D9, 416 (1974).

16. D.J. Gross, and F. Wilczek, Phys. Rev. D9, 980 (1974).

17. E.G. Floratos, D.A. Ross, and C.T. Sachrajda, Nucl. Phys. B129, 66 (1977) and Erratum, Nucl. Phys. B139, 545 (1978).

18. G. Curci, W. Furmanski, and R. Petronzio, Th.2815-CERN (1980).

19. E.G. Floratos, R. Lacaze, and C. Kounnas, Saclay preprint 77/80.

20. E.G. Floratos, D.A. Ross, and C.T. Sachrajda, Nucl. Phys. B152, 493 (1979).

21. E.G. Floratos, R. Lacaze, and C. Kounnas, Saclay preprint 83/80.

22. W.A. Bardeen, A.J. Buras, D.W. Duke and T. Muta, Phys. Rev. D18, 3998 (1978).

23. A. Gonzales-Arroyo, C. Lopez, and F.J. Yndurain, Nucl. Phys. B153, 161 (1979); Nucl. Phys. B166, 429 (1980).

24. M. Bace, Phys. Lett. 78B, 132 (1978).

25. W. Celmaster and R.J. Gonsalves, Phys.Rev. Lett. 42, 1435 (1979) and Phys. Rev. D20, 1420 (1979).

26. R. Barbieri, L. Caneschi, G. Curci and E. D'Emilio, Phys. Lett. 81B, 207 (1979).

27. A. Hasenfratz and P. Hasenfratz, CERN preprint TH2827 (1980); R. Dashen and D.J. Gross, Princeton preprint, 80-0583 (1980).

28. A.J. Buras, FERMILAB-Pub-80/43-THY (1980).

29. K. Harada and T. Muta, Phys. Rev. D22, (1980).

30. W. Celmaster and D. Sivers, ANL-HEP-PR-80-30.

31. P.M. Stevenson, Madison preprints DOE-ER/0881-153 (1980) and DOE-ER/0881-155 (1980).

32. M. Moshe, Phys. Rev. Lett. 43, 1851 (1979).

33. L.F. Abbott, Phys. Rev. Lett. 44, 1569 (1980).

34. Similar conclusion has been reached by H. Bohr and T. Muta, private communication.

35. D.A. Ross, and C.T. Sachrajda, Nucl. Phys. B149, 497 (1979).

36. It is slightly larger in the singlet sector. D.W. Duke, private communication.

37. G. Altarelli, R.K. Ellis, and G. Martinelli, Nucl. Phys. B143, 521 (1978).

38. M.R. Pennington and G.G. Ross, Phys. Letters 86B, 331 (1979).

39. D.W. Duke and R.G. Roberts, Nucl. Phys. B166, 243 (1980).

40. A. Para and C.T. Sachrajda, Phys. Letters 86B, 331 (1979).

41. H.L. Anderson, et al., FERMILAB-Pub-79/30-EXP.

42. P.C. Bosetti, et al., Nucl. Phys. B 142, 1 (1978). J.G.H. De Groot, et al., Z. Phys. C1, 143 (1979). S.M. Heagy, et al., Univ. of Pennsylvania preprint (1980).

43. B.A. Gordon, et al., Phys. Rev. Lett. 41, 615 (1978).

44. For a recent review of ν data see N. Schmitz, MPI-PAE/EXP-EL89 (1980).

45. W.A. Bardeen, and A.J. Buras, Phys. Lett. B86, 61 (1979).

46. M. Haruyama, and A. Kanazawa, Asahikawa preprint (1980).

47. L. Baulieu and C. Kounnas, Nucl. Phys. B141, 423 (1978); I. Kodaira and T. Uematsu, Nucl. Phys. B141, 497 (1978).

48. G. Altarelli, R.K. Ellis, and G. Martinelli, Nucl. Phys. B157, 461 (1979).

49. A. Biaℓas, and A.J. Buras, Phys. Rev. D21, 1825 (1980).

50. G. Altarelli, and G. Parisi, Nucl. Phys. B126, 298 (1977).

51. A.J. Buras, and K.J.F. Gaemers, Nucl. Phys. B132, 249 (1978) ; A.J. Buras, Nucl. Phys. B125, 125 (1977).

52. See the talks by H. Weerts and I.G.H. De Groot in the Proceedings of the 1980 International Conference on High Energy Physics, Madison (1980).

53. T. Gottschalk, ANL-HEP-PR-80-35 (1980).

54. L. Baulieu, E.G. Floratos and C. Kounnas, CEN Saclay preprint DPh-T/138, to be published in Nucl. Phys. B.

55. R.T. Herrod and S. Wada, Univ. of Cambridge preprint, HEP 80/6.

56. A. Gonzalez-Arroyo and C. Lopez, CERN preprint TH.2734 (1979); C. Lopez and F.T. Yndurain, Nucl. Phys. B171, 231 (1980). The latter paper dicusses the $x \to 0,1$ behavior of structure functions.

57. P. Aurenche, N.G. Fadeev, J. Lindfors, N.B. Skachokov, Y.I. Ivanshin, and D.A. Ross, Ref. TH2887-CERN, M. Haruyama and A. Kanazawa, Asahikawa preprint (1979).

58. D.J. Gross, Phys. Rev. Lett. 32, 1071 (1974).

59. K. Kato, and Y. Shimizu, Univ. of Tokyo preprint UT-336.

60. R.P. Feynman, R. Field and D.A. Ross, unpublished. (See ref. 7 for details). J. Wosiek and K. Zalewski, Warsaw University preprint, TPJU-3/80 (1980).

61. R.G. Roberts, J. Wosiek, and K. Zalewski, in preparation.

62. I. Kodaira, S. Matsuda, K. Sasaki and T. Uematsu, Nucl. Phys. B159, 99 (1979). I. Kodaira, S. Matsuda, T. Muta, and T. Uematsu, Phys. Rev. D20, 627 (1979); T. Muta, Phys. Lett. 89B, 413 (1980).

63. M.A. Ahmed and G.G. Ross, Phys. Lett. B56, 385 (1975) and Nucl. Phys. B111, 441 (1976).

64. R.L. Jaffe and G.G. Ross, Phys. Letters 93B, 313 (1980).

65. A. De Rujula and F. Martin, MIT Preprint CTP No. 851 (1980).

66. P.W. Johnson and W.K. Tung, contribution to International Conference, Neutrino 79, Bergen, Norway. J. Sheiman, Berkeley Preprint, LBL-10272 (1980).

67. L.F. Abbot, and M. Wise, SLAC-Pub-2482 (1980).

68. L.F. Abbott, E.L. Berger, R. Blankenbecler and G. Kane, Phys. Letters 88B, 157 (1979).

69. W.B. Atwood, SLAC-Pub-2428 (1979).

70. C. Lopez and F.T. Yndurain, Madrid University preprint FTUAM/80-6.

71. E.M. Haacke, Case Western Reserve University preprint.

72. P. Norton (EMC Collaboration), Proceedings of the XXth Conf. on High Energy Physics, Madison, Wisconsin (1980); See also D. Bollini et al. (BCDMS collaboration), CERN preprint, CERN/EP 80-133.

73. R.C. Ball, et al., Phys. Rev. Lett. 42, 866, (1979).

74. R. Jost, and T.M. Luttinger, Helv. Phys. Acta 23, 201 (1950); T. Appelquist and H. Georgi, Phys. Rev. D8, 4000 (1973); A. Zee, Phys. Rev. D8, 4038 (1973).

75. M. Dine and J. Sapistein, Phys. Rev. Lett. 43, 668 (1979); K.G. Chetyrkin, A.L. Kataev and F.V. Tkachov, Phys. Lett. 85B, 277 (1979).

76. W. Celmaster and R.J. Gonsalves, Phys. Rev. Lett. 44, 560 (1980) and Phys. Rev. D21, 3112 (1980).

77. E. Poggio, H. Quinn and S. Weinberg, Phys. Rev. D13, 1958 (1976); R.G. Moorhouse, M.R. Pennington and G.G. Ross, Nucl. Phys. B124, 285 (1977); R. Barbieri and R. Gatto, Phys. Lett. 66B, 181 (1977); R. Shankar, Phys. Rev. D15, 755 (1977).

78. R.M. Barnett, M. Dine and L. McLerran, Phys. Rev. D22, 594 (1980).

79. E. Witten, Nucl. Phys. B120, 189 (1977).

80. W.A. Bardeen and A.J. Buras, Phys. Rev. D20, 166 (1979).

81. D.W. Duke and J.F. Owens, Florida State University preprint 800415 (1980).

82. W. Wagner, to appear in the proceedings of the XXth International Conf. on High Energy Physics, Madison (1980).

83. C.H. Llewellyn-Smith, Phys. Lett. B79, 83 (1978); R.T. DeWitt, L.M. Jones, J.D. Sullivan, D.E. Willen and H.W. Wyld,Jr., Phys. Rev. D19, 2046 (1979).

84. See, for instance, S.J. Brodsky, T. De Grand, J.F. Gunion and J. Weis, Phys. Rev. D19, 1418 (1979); K. Kajantie, Helsinki University preprints HU-TFT-78-30, HU-TFT-79-5; W.R. Frazer and J.F. Gunion, Phys. Rev. D20, 147 (1979).

85. C.T. Hill and G.G. Ross, Nucl. Phys. B148, 373 (1979).

86. M.K. Chase, Nucl. Phys. B167, 125 (1980).

87. A.C. Irving and D.B. Newland, University of Liverpool preprint, LTH 58 (1980); F. Delduc, M. Gorudin, El Ghali Oudrhiri-Safiani, PAR-LPTHE-80-04, 80-07 (1980); A. Voudas, Manchester Univ. Preprint M/C TH 79/6 (1979).

88. R. Barbieri, E. d'Emilio, G. Curci and E. Remiddi, Nucl. Phys. B154, 535 (1979).

89. A. Duncan and A.H. Mueller, Phys. Lett. 93B, 119 (1980).

90. T. Appelquist and H.D. Politzer, Phys. Rev. D12, 1404 (1975).

91. W. Celmaster and D. Sivers, ANL-HEP-PR-80/29 (1980); See also G. Parisi and R. Petronzio, CERN preprint TH-2804, (1980); W. Celmaster, in Proceedings of the XXth International Conf., Madison (1980).

92. R. Barbieri, M. Caffo, R. Gatto, and E. Remiddi, UGVA-DPT 1980/06-247.

93. W. Celmaster, ANL-HEP-80-60; G.Greenberg, Cornell Univ. preprint (1980).

94. T. Appelquist, R. Barnett, and K. Lane, Ann. Rev. Nucl. and Part. Sci. 28, 387 (1978); J.D. Jackson, C. Quigg and J.L. Rosner, Proceedings of the 19th International Conference on High Enrgy Physics, Tokyo 1978, edited by S. Homma, M. Kawaguchi and H. Miyazawa (International

Academic Printing Co., Ltd., Japan) p.391 (1979).

95. F. Bloch and A. Nordsieck, Phys. Rev. 52, 54 (1937).

96. D.R. Yennie, S.C. Frautschi and H. Suura, Ann. Phys. (NY) 13, 379 (1961); G. Grammer and D.R. Yennie, Phys. Rev. D8, 4352 (1973).

97. T. Kinoshita, J. Math. Phys. 3, 650 (1962).

98. T.D. Lee and M. Nauenberg, Phys. Rev. 133, 1549 (1964).

99. G. Sterman and S. Weinerg, Phys. Rev. Lett. 39, 1436 (1977).

100. I.G. Halliay, Nucl. Phys. B103, 343 (1976).

101. H.D. Politzer, Phys. Lett. 70B, 430 (1977); Nucl. Phys. B129, 301 (1977).

102. C.T. Sachrajda, Phys. Lett. 73B, 185 (1978); Phys. Lett. 76B, 100 (1978).

103. W. Furmanski, Phys. Lett. 77B, 312 (1978).

104. Y. Kazama and Y.P. Yao, Phys. Rev. Lett. 41, 611 (1978); Phys. Rev. D19, 3111, 3121 (1979).

105. W.B. Frazer and J.F. Gunion, Phys. Rev. D19, 2447 (1979).

106. C.H. Llewellyn Smith, Acta Phys. Austriaca Suppl. XIX, 331 (1978).

107. A.V. Radyushkin, Phys. Lett. 69B, 245 (1977).

108. D. Amati, R. Petronzio and G. Veneziano, Nucl. Phys. B140, 54 (1978) and B146, 29 (1978).

109. R.K. Ellis, H. Georgi, M. Machacek, H.D. Politzer and G.G. Ross, Phys. Lett. 78B, 281 (1978); Nucl. Phys. B152, 285 (1979).

110. S. Libby and G. Sterman, Phys. Lett. 78B, 618 (1978); Phys. Rev. D18, 3252, 4737 (1978).

111. G. Sterman, Phys. Rev. D19, 3135 (1979); Phys. Rev. D17, 2773, 2789 (1978).

112. A.H. Mueller, Phys. Rev. D18, 3705 (1978).

113. S. Gupta and A.H. Mueller, Phys. Rev. D20, 118 (1979).

114. S. Gupta, Phys. Rev. D21, 984 (1980).

115. A. Duncan, S. Gupta, and A.H. Mueller, CU-TP-179 (1980).

116. I. Antoniadis, L. Baulieu and C. Kounnas, LPTENS, 79/28 (1979).

117. I. Antoniadis and C. Kounnas, Ecole Polytechnique preprint (1980).

118. E.G. Floratos, contribution to this symposium and references therein.

119. Frenkel and J.C. Taylor, Nucl. Phys. B116, 185 (1976).

120. J. Kripfganz, Phys. Lett. B82, 79 (1979).

121. J.F. Owens, Phys. Lett. 76B, 85 (1978); T. Uematsu, Phys. Lett. 79B, 97 (1978).

122. A.J. Buras, in "Quantum Flavordynamis, Quantum Chromodynamics, Quantum Chromodynamics and Unified Theories", ed. K.T. Mahanthappa and J. Randa, Plenum Press, P.349 (1980).

123. B. Humpert and W.L. Van Neerven, Phys. Lett. 89B, 69 (1979); and CERN preprints, CERN-TH-2785, 2805 (1980).

124. G.T. Bodwin, C.Y. Lo, J.D. Stack and J.D. Sullian, ILL-TH-80-2.

125. J. Ambjørn and N. Sakai, Nordita 80/14 (1980).

126. J. Kripfganz, McGill preprint, 79-0912 (1979).

127. K. Harada, T. Kaneko and N. Sakai, Nucl. Phys. B155, 169 (1978).

128. N. Sakai, Phys. Lett. 85B, 67 (1979).

129. J. Kubar-Andre and F.E. Paige, Phys. Rev. D19, 221 (1979).

130. G. Altarelli, R.K. Ellis, G. Martinelli and S.Y. Pi, Nucl. Phys. B160, 30 (1979).

131. R. Baier and K. Fey, Z. Phys. C2, 339 (1979).

132. B. Humpert and W.L. Van Neerven, Phys. Lett. 84B, 327 (1979), Phys. Lett. 85B, 293 (1979).

133. A.P. Contogouris and J. Kripfganz, Phys. Lett. B84, 473 (1979); Phys. Rev. D19, 2207 (1979).

134. V. Gribov and L. Lipatov, Sov. J. Phys. 15, 675 (1972).

135. L. Baulieu, E.G. Floratos, C. Kounnas, Phys. Lett. 89B, 84 (1979).

136. J. Kalinowski, K. Konishi and T.R. Taylor, CERN preprint 2902.

137. See refs. 19 and 21.

138. Recall that the $\overline{MS}$ scheme as defined in [22] is obtained from t'Hooft's MS scheme by removing $\ln 4\pi-\gamma_E$ terms from $B^S_{k,n}$ but keeping $\gamma^{(1)n}_{NS}$ unchanged. In higher orders, where powers of $\gamma^{(1),n}_{NS}$ and $B^S_{k,n}$ appear (see 2.22) more care is needed.

139. A.J. Buras and N. Sakai, unpublished.

140. J. Blietschau et al., Phys. Lett. 87B, 281 (1979); Proc. Intern. Conf. High-Energy Phys., Geneva, Vol.1, p.151 (1979); Proc. Neutrino 79, Bergen, Vol.2, p. 499 (1979). W.G. Scott, Proc. 14th Recontre de Moriond, Vol.I, p.307 (1979); Proc. Neutrino 79, Bergen, Vol.2, p.533 (1979).

141. G. Parisi, Phys. Lett. 90B, 295 (1980).

142. C.P. Korthals-Altes and E. de Rafael, Nucl. Phys. B106, 237 (1976); Nucl. Phys. B125, 275 (1977).

143. Y.L. Dokshitzer, Soviet Physics, JETP 46, 461 (1977); J.M. Cornwall and G. Tiktopoulos, Phys. Rev. D13, 3370 (1976).

144. A.H. Mueller, Phys. Rev. D20, 2037 (1979).

145. G. Curci an M. Greco, Phys. Lett. 92B, 175 (1980); M. Greco, Frascati preprint, LNF-80/18(P) (1980).

146. D. Amati, A. Bassetto, M. Ciafaloni, G. Marchesini and G. Veneziano, CERN-TH-2831 (1980); M. Ciafaloni, Phys. Lett. 95B, 113 (1980). A. Bassetto, LPTHE 80/13 (1980).

147. L. Caneschi, Univ. of Pisa preprint 80-0559 (1980).

148. V. Sudakov, Sov. Phys. JETP 3, 65 (1956).

149. W. Furmanski, R. Petronzio and S. Pokorski, Nucl. Phys. B155, 253 (1979).

150. A.P. Contogouris and J. Kripfganz, Phys. Rev. D20, 2295 (1979).

151. A.N. Schellekens and W.L. Van Neerven, Phys. Rev. D21, 2619 (1980) and THEF-NYM-79-17 (1979).

152. M. Chaichian, M. Hayashi and T. Honkarante, Helsinki Univ. preprint HU-TFT-80.9.

153. P. Aurenche and J. Lindfors, TH.2786-CERN (1980).

154. A.P. Contogouris, L. Marleau and S. Papadopoulos, McGill preprint 80-0352 (1980); A.P. Contogouris, J. Kripfganz, L. Marleau, S. Papadopoulos, McGill preprint 80-0355 (1980).

155. R.K. Ellis, M.A. Furman, H.G. Haber and I. Hinchlife, LBL-10304 (1980).

156. R. Cutler and D. Sivers, Phys. Rev. D16, 679 (1977).

157. B.L. Combridge, J. Kripfganz and J. Ranft, Phys. Lett. B70, 234 (1977).

158. See refs. 102 and 103 and 7 for a general discussion of large p processes in QCD.

159. M.A. Furman, Columbia preprint, CU-TP-182.

160. R.K. Ellis, D.A. Ross and A.E. Terrano, CALT-68-783 and CALT-68-785.

161. See refs. 225 and 228.

162. R. Doria, J. Frenkel and J.C. Taylor, Nucl. Phys. B168, 93 (1980).

163. C. Di'Lieto, S. Gendron, I.G. Halliday and C.T. Sachrajda, ICTP/79-80/47; SHEP 79/80-6.

164. A. Andrasi, M. Day, R. Doria, J. Frenkel and J.C. Taylor, Oxford University Preprint 37/80 (1980).

165. A. Andrasi, M. Day, R. Doria, J.D. Taylor, C. Carneiro, J. Frenkel and M. Thomas, to appear in the proceedings of the XXth International Conf. on High Energy Physics, Madison (1980).

166. P. Cvitanovic and P. Scharbach, private communication.

167. D.H. Perkins, Proc. Neutrino 79, Bergen, Vol.1, p.429 (1979).

168. N. Schmitz, Max Planck Institute preprints MPI-PAE/Exp. EL.88,89 (1980).

169. E.L. Berger and S.J. Brodsky, Phys. Rev. Lett. 42, 940 (1979). G.R. Farrar and D.R. Jackson, Phys. Rev. Lett. 35, 1416 (1975).

170. E.L. Berger, Phys. Lett. 89B, 241 (1980), and SLAC-Pub 2362 (1979); E.L. Berger, T. Gottschalk and D. Sivers, ANL-HEP-PR-80-58 (1980).

171. S. Gottlieb, Nucl. Phys. 139, 125 (1978).

172. M. Okawa, Univ. of Tokyo preprint, UT-337 (1980).

173. L.F. Abbott and R.M. Barnett, Ann. Phys. 125, 276 (1980).

174. D. Perkins, unpublished.

175. D.W. Duke and R.G. Roberts, Rutherford Lab. preprint, RL-80-016 (1980).

176. M.R. Pennington and G.G. Ross, Oxford preprint (1980).

177. A. Donnachie and P.V. Landshoff, M/C TH 80/11 and DAMTP 80/6 (1980).

178. R. Blankenbecler, S.J. Brodsky and J.F. Gunion, Phys. Rev. D18, 900 (1978); P.V. Landshoff and J.C. Polkinghorne, Phys. Rev. D10, 891 (1974); M.K. Chase and W.J. Stirling, Nucl. Phys. B133, 157 (1978).

179. S.J. Brodsky, R.R. Horgan and W.E. Caswell, Phys. Rev. D18, 2415 (1978); M. Chase, Nucl. Phys. B145, 189 (1978).

180. H.D. Politzer, CALT-68-765 and contribution to this symposium.

181. M. Hagenauer, et al., CERN/EP/80-124 (1980).

182. S.J. Brodsky, contribution to this symposium.

183. A. Duncan, contribution to this symposium (CU-TP-187).

184. S.J. Brodsky and G.R. Farrar, Phys. Rev. Lett. 31, 1153 (1973); Phys. Rev. D11, 1309 (1975).

185. V.A. Matveev, R.M. Muradyan and A.V. Tavkelidize, Lett. Nuovo Cimento 7, 719 (1973).

186. P.V. Landshoff, Phys. Rev. D10, 1024 (1974).

187. S.J. Brodsky and G.P. Lepage, Phys. Lett. 87B, 359 (1979).

188. G. Farrar and D. Jackson, Phys. Rev. Lett. 43, 246 (1979).

189. A.V. Efremov and A.V. Radyushkin, Dubna preprints JINR-E2-11535, 11983 and 12384.

190. G. Parisi, Phys. Lett. 84B, 225 (1979).

191. S.J. Brodsky, Y. Frishman, G.P. Lapage and C.T. Sachrajda, Phys. Lett. 91B, 239 (1980).

192. S.J. Brodsky and G.P. Lapage, Phys. Rev. Lett. 43, 545 (1979).

193. A.Duncan and A. Mueller, Phys. Lett. 90B, 159 (1980).

194. A. Duncan and A.H. Mueller, Phys. Rev. D21, 1636 (1980).

195. M. Peskin, Phys. Lett. 88B, 128 (1979).

196. I.G. Aznauryan, S.V. Esaybegyan and N.L. Terisaakyan, Phys. Lett. 90B, 151 (1980).

197. G.P. Lepage and S.J. Brodsky, refs. 8,187,191,192 and in particular SLAC-PUB-2478, where a very extensive list of further references and details of calculations can be found.

198. P.V. Landshoff and D.J. Pritchard, Cambridge preprint DAMTP 80/04.

199. V. Sudakov, Sov. Phys. JETP 3, 65 (1956).

200. C. Bebek, et al., Phys. Rev. D13, 25 (1976).

201. M.D. Mestayer, SLAC Report 214 (1978) and references therein.

202. P.V. Landshoff and J.C. Polkinghorne, Phys. Lett. 44B, 393 (1973). See also Section 7 of ref.8.

203. A.H. Mueller, in Proceedings of the Johns Hopkins Workshop on Current Problems in Particle Theory, Bad Honnef/Bonn, p.35 (1980).

204. G. Altarelli, G. Parisi and R. Petronzio, Phys. Lett. 76B, 351 (1978); Phys. Lett. 76B, 356 (1978).

205. H. Fritzsch and P. Minkowski, Phys. Lett. 73B, 80 (1978).

206. C. Michael and T. Weiler, contribution to the XIIIth Recontre de Moriond, Les Arcs, France (1978).

207. K. Kajantie and R. Raitio, Nucl. Phys. B139, 72 (1978).

208. K. Kajantie, J. Lindfors and R. Raitio, Phys. Lett. 74B, 384 (1978); J. Cleymans and M. Kuroda, Phys. Lett. 80B, 385 (1979); J.C. Collins, Phys. Rev. Lett. 42, 291 (1979).

209. K. Kajantie and J. Lindfors, Nucl. Phys. B146, 465 (1978).

210. F. Halzen and D. Scott, Phys. Rev. D18, 3378 (1978); Phys. Rev. D19, 216 (1979).

211. E.L. Berger, ANL-HEP-PR-78-12, ANL-HEP-CP-80-24.

212. For a nice review of data see R. Stroynowski, SLAC-PUB-2402 (1980).

213. Yu L. Dokshitzer, D.I. Dyakonov and S.I. Troyan, Phys. Lett. 78B, 290 (1978); 79B, 269 (1978).

214. G. Parisi and R. Petronzio, Nucl. Phys. B154, 427 (1979).

215. C.Y. Lo and J.D. Sullivan, Phys. Lett. 86B, 327 (1979).

216. S.D. Ellis and W.J. Stirling, preprint RLO-1388-821 (1980).

217. D.E. Soper, OITS-134 (1980).

218. D.E. Soper and J.C. Collins, to be published in the Proceedings of the 20th International Conference on High Energy Physics, Madison, 1980; see also J.C. Collins, Princeton University preprint (1980) and A.H.Mueller [144].

219. J.C. Collins, Phys. Rev. D21, 2962 (1980) and a talk to be published in the Proceedings of the 20th International Conference on High Energy Physics, Madison, 1980.

220. H.F. Jones and J. Wyndham, Preprints ICTP/79-80/41 and ICTP/79-80/48 (1980); N.S. Craigie and H.F. Jones, Nucl. Phys. B172, 59 (1980).

221. J.B. Kitterick, ILL(TH)-80-22 (1980).

222. C.L. Basham, L.S. Brown, S.D. Ellis and S.T.Love, Phys. Lett. 85B, 297 (1979); G.C. Fox and S. Wolfram, Nucl. Phys. B149, 413 (1979) and CALT-68-723 (1979).

223. W. Marquardt and F. Steiner, DESY preprint 80/1 (1980).

224. Yu. L. Dokshitzer and D.I. Dyakonov, DESY L-Trans-234 (1979).

225. G. Schierholz, DESY 79/71 (1979) and contribution to this symposium.

226. J. Wosiek and K. Zalewski, Nucl. Phys. B161, 294 (1979).

227. P. Binetruy, Phys. Letters 91B, 245 (1980).

228. A. Ali, J.G. Korner, Z. Kunszt, J. Willrodt, G. Kramer, G. Schierholz and E. Pietarinen, Phys. Lett. 82B, 285 (1979) and Nucl. Phys. B167, 454 (1980); K.J.F. Gaemers and J.A.M. Vermaseren, TH-2816 CERN.

229. A. Ali, E. Pietarinen, G. Kramer and J. Willrodt, Phys. Lett. 93B, 155 (1980).

230. R. Kajantie and E. Pietarinen, Phys. Lett. 93B, (269) 1980.

231. A. Bassetto, M. Ciafaloni and G. Marchesini, Nuclear Phys. B163, 477 (1980), and Phys. Letters 83B, 207 (1979).

232. D. Amati and G. Veneziano, Phys. Letters 83B, 87 (1979).

233. K. Konishi, A. Ukawa, and G. Veneziano, Nuclear Phys. B157, 45 (1979); Phys. Letters 78B, 243 (1978); Phys. Letters 80B, 259 (1979).

234. J. Kalinowski, K. Konishi, P. Scharback and T.R. Taylor, in preparation; J. Kalinowski and T.R. Taylor, Warsaw University preprint IFT/11/1980.

235. C.H. Lai, J.L. Petersen and T.F. Walsh, NBI-HE-80-3.

236. G.C. Fox and S. Wolfram, Caltech-68-755 (1979).

237. H. Fritzsch and P. Minkowski, Phys. Letters 69B, 316 (1977).

238. See for instance J.F. Owens, Phys. Rev. D21, 54 (1980) and references therein.

239. F. Halzen and D.M. Scott, Phys. Lett. 80B, 410 (1979) and references therein.

240. F.M. Renard, Lectures given at the International School of Elementary Particle Physics, Kupari-Dubrovnik, PM/79/15 (1979).

241. P.W. Johnson and W.K. Tung, Illinois Institute of Technology preprint (1980).

242. R.P. Bajpai, M. Noman and R. Ramachandran, Indian Institute of Technology preprint, (1980).

243. J.T. Donohue and S. Gottlieb, ANL-HEP-PR-80-42 (1980).

Figure Captions

Fig. 1 Typical diagrams which enter the calculation of $B^{NS}_{k,n}$: a) diagrams contributing to the virtual Compton amplitude, b) diagrams contributing to the matrix elements of non-singlet operators.

Fig. 2 Coefficients $R^{NS}_{2,n}$ as functions of n for the $\overline{MS}$ and MOM schemes and four effective flavors.

Fig. 3 $M^{NS}_2(n,Q^2)$ as given by Eq. (2.10) as functions of Q^2 for $\Lambda_{\overline{MS}}=0.30$ GeV and $\Lambda_{MOM}=0.55$ GeV.

Fig. 4 The effective coupling constant $\alpha(Q^2)$ for the $\overline{MS}$ and MOM schemes with Λ_i of Eq. (2.17). For comparison also $\alpha(Q^2)$ in the leading order approximation is shown.

Fig. 5 "Empirical" relation between $\Lambda_{\overline{MS}}$ and Λ_{MOM} (dashed curves) obtained by fitting $M^{NS}_2(n,Q^2)$ of Eq. (2.10) in the MOM scheme to the corresponding moments in the $\overline{MS}$ scheme. The fit has been done for $2 \leq n \leq 8$ and $10\ GeV^2 \leq Q^2 \leq 200\ GeV^2$. The solid line represents the exact relation (2.16).

Fig. 6 $1 + \alpha(Q^2)/4\pi\ R^{NS}_{2,n}$ as functions of n, for $Q^2=10\ GeV^2$, $Q^2=100\ GeV^2$, and the Λ_i values of Eq. (2.17).

Fig. 7 $1 + R^{NS}_{2,n}(Q^2)/(\beta_0 \ln(Q^2/\Lambda_i^2))$ as functions of n for $Q^2=10\ GeV^2$, $Q^2=100\ GeV^2$ and the Λ_i values of Eq. (2.17).

Fig. 8 a) Diagram entering the calculation of γ^{β}_n of Eq. (2.24) and corresponding to $q \to \bar{q}+qq$ transition.

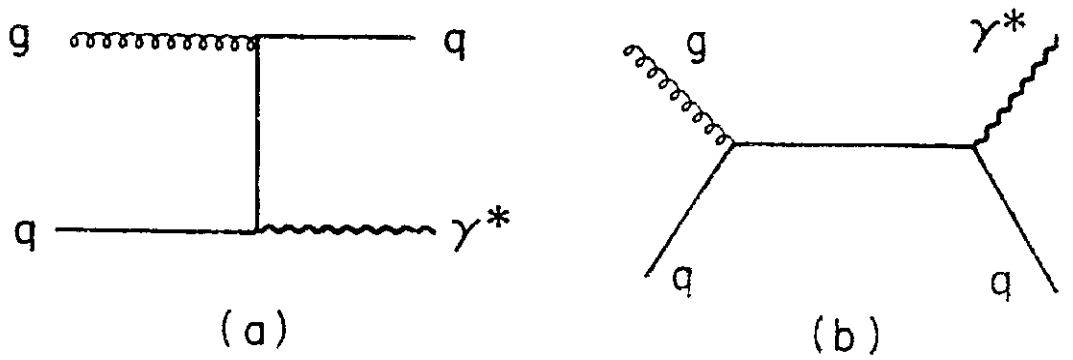

Fig. 26

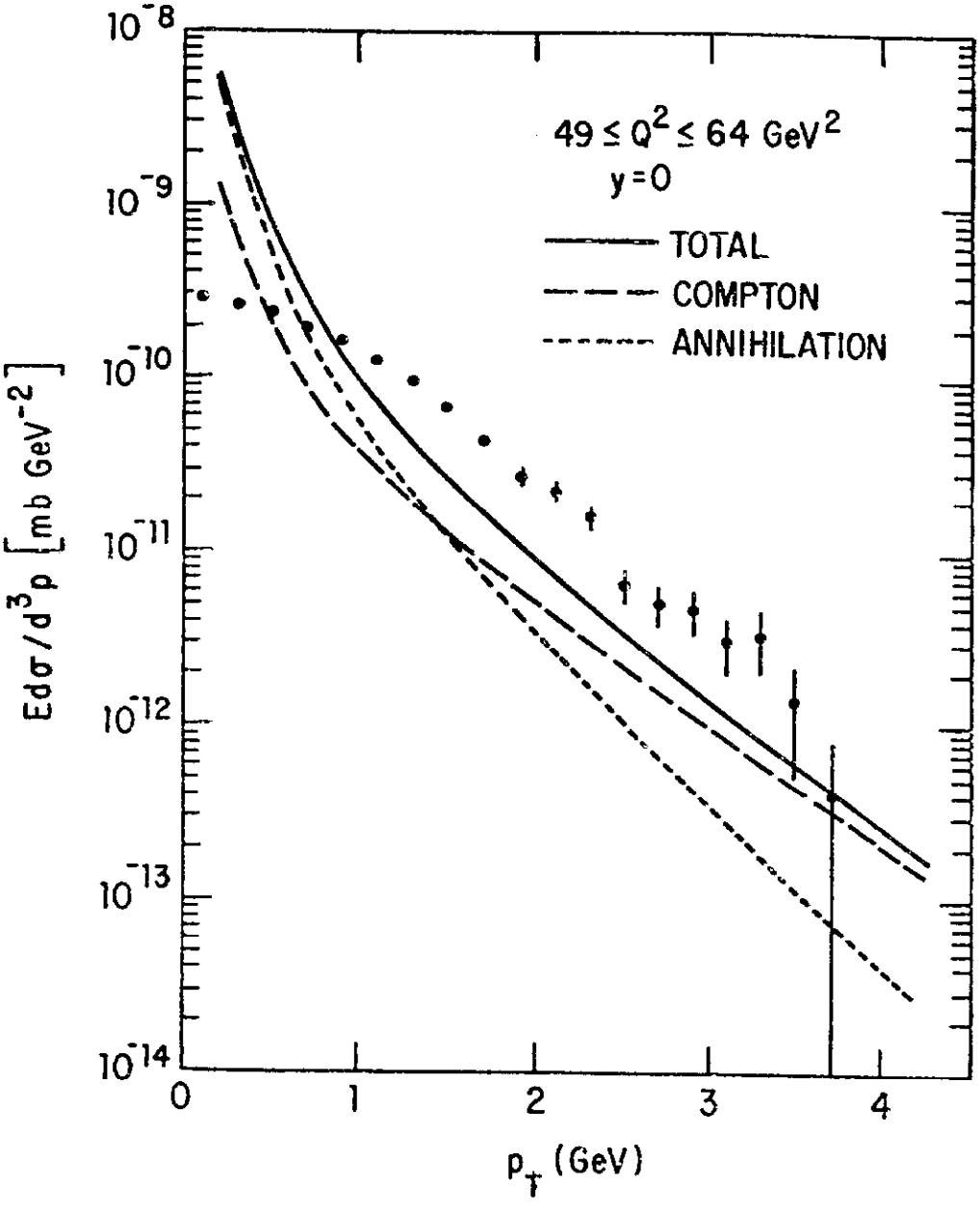
10^{-8}
10^{-9}
10^{-10}
10^{-11}
10^{-12}
10^{-13}
10^{-14}
$Ed\sigma/d^3p$ [mb GeV^{-2}]
$49 \leq Q^2 \leq 64$ GeV^2
$y = 0$
TOTAL
COMPTON
ANNIHILATION
0
1
2
3
4
p_T (GeV)

Fig. 27

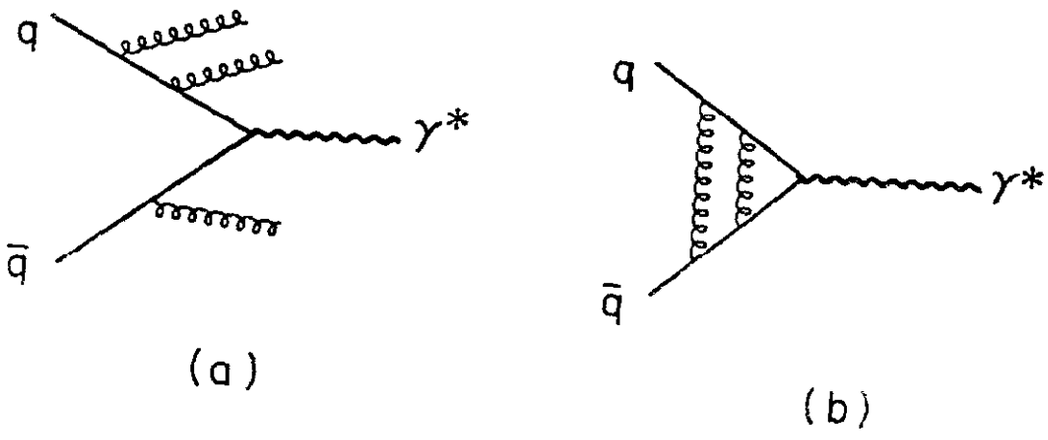

Fig. 28